AD-A127 595 A STUDY TO EVALUATE DIGITAL ACOUSTIC LINKS FOR SONOBUOY APPLICATIONS(U) BELL TELEPHONE LABS INC WHIPPANY NJ 30 MAR 83 N62269-83-M-3006 1/1

UNCLASSIFIED F/G 9/6 NL

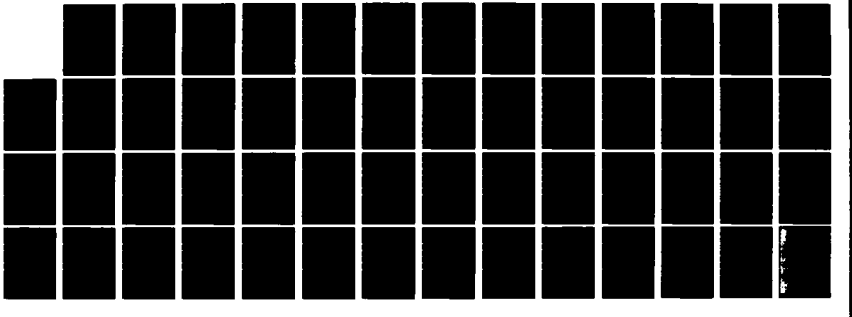

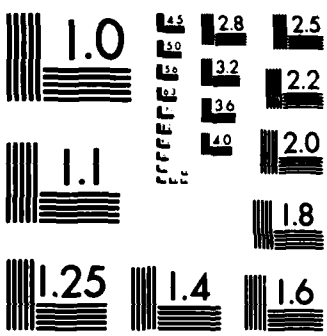

# A STUDY TO EVALUATE
# DIGITAL ACOUSTIC LINKS
# FOR SONOBUOY APPLICATIONS

March 30, 1983

Prepared by Bell Laboratories
Whippany Road, Whippany, N.J. 07981
on behalf of Western Electric
under Contract N62269-83-M-3006 for
the Naval Air Development Center

*ABSTRACT*

A study has been performed for the Naval Air Development center, under Contract N62269-83-M-3006, to assess the applicability of digital acoustic-links for telemetry of data between sonobuoy modules. Specifically, operational range, power required, transmission frequency and modulation format were considered. The primary conclusion obtained is that a low power digital acoustic link is feasible for transmission rates up to a few kilobits per second and ranges to several kilometers. However, to achieve this performance in a fading acoustic environment, diversity, either spatial or frequency, is required.

## 1. INTRODUCTION

This document reports on work performed under Contract N62269-83-M-3006 for the Naval Air Development Center. This study addresses the feasibility of using a digital acoustic-link, subject to constraints on size and power consumption imposed by the sonobuoy environment, to telemeter data between sonobuoy modules.

Although acoustic telemetry links have found a wide variety of applications in oceanic research and engineering [1] [2] [3] [4] [5] [6] [7] [8] [9], the extension of this technology to sonobuoys has not occurred. This is primarily due to the fact that, until recently, sonobuoys have been "shallow" and had relatively short lives, characteristics well matched to cable links. However, recent interest has focused on deep or moored buoys with relatively long lives. It has been found that variable depth wire telemetry links suffer a number of inadequacies when required to operate in these systems. Indeed, some deployment scenarios may not permit the use of a surface radio transmitter permanently tethered to a deep sensor package. This study explores the feasibility of using a digital acoustic link to transmit processed data between sonobuoy modules, in place of the traditional wire link. Since the concept of an underwater acoustic communications link is not new, Section 2 will survey previous work in this area. Section 3 presents the current model with emphasis on how it extends previous work, specifically, time dependent fluctuations are considered and a particular modulation format, Frequency Shift Key (FSK) modulation is employed. Results derived from this model are presented in Section 4. The primary conclusion obtained is that a low power digital acoustic

link is feasible for transmission rates up to a few kilobits per second and ranges to several kilometers. However, to achieve this performance in a fading acoustic environment, diversity, either spatial or frequency, is required.

## 2. PREVIOUS WORK

Underwater digital acoustic communication has been studied for many years, both theoretically and experimentally. The usual motivation for this work has been long range communication [4], although the relatively recent surge of interest in underwater work vehicles has sparked study of lower power, shorter range systems.

While not directly applicable to system design, the previous studies do highlight relevant considerations. The usual approach taken in these studies is to derive signal-to-noise ratios from the SONAR equation, and then estimate channel capacity from the Shannon limit [10] [11]:

$$C = B * \log_2(1 + S / N)$$

where C is the channel capacity in bits/s, B is the bandwidth and S/N is the signal to noise power ratio. Since assumptions of optimal coding and long time delays are implicit in this analysis, the predicted capacity is much greater than can be achieved in practice. A more realistic estimate can be obtained by reducing the signal to noise ratio by a factor of 1/7 [12], equivalent performance thus requiring an 8.4 dB increase in power.

Regardless of the correction factor, the form of this equation is instructive. Note that the channel capacity varies directly with the available bandwidth and only logarithmically with the SNR. Available bandwidth, however, is severely constrained in underwater acoustic transmission, on the high frequency side by volume absorption, and on the low frequency side by increasing noise and increasing transmitter size required to achieve a given directivity index. Thus efficient bandwidth utilization is important in these systems.

As expected, the maximum data rates measured at sea are well below the Shannon limit. Painter [6], for example, was able to transmit data over several kilometers at a maximum rate of 1500 bits per second. He reports that,

at least in part, time dependent fluctuations, resulting in variations of the optimum decision threshold, precluded higher transmission rates. More recently, Quazi et al. [13] have achieved data rates of several kilobits per second to ranges of several kilometers. Once again, time dependent fluctuations were observed. Data from this work will be discussed below. Other measurements [4] [5] [6] [7], while achieving equivalent or superior range performance, have done so at the expense of data rate, even as low as 30 bits per second. In general, measurements made to date have not tried to minimize power consumption (an important consideration in sonobuoy systems), often requiring tens or hundreds of watts.

## 3. THE CURRENT MODEL

The current model was developed to study the application of acoustic data-links to sonobuoys, subject to their power and size constraints. This model, too, derives signal-to-noise ratios from the SONAR equation. It differs from the previous work in the choice of parameters to be consistent with sonobuoy constraints. Additionally, the derived SNRs are subsequently employed in performance predictions for a specific modulation scheme, Frequency Shift Key or FSK, in a fading acoustic environment.

### 3.1 Transmission

The current calculations, for a receiver located directly above the transmitter, assume a circular piston radiator transmitter producing a beam pattern similar to that shown in Figure 1, where the angle between -3 dB points is 30 degrees. The choice of this transducer was motivated both by calculational simplicity and by considering size limitations imposed by sonobuoy containers. Of course, other directional transducers could be considered; Figure 2, for example, shows the beam pattern for a 10 element linear array with binomial weighting and quarter wave spacing. Use of such an array eliminates side-lobe radiation, improving covertness and minimizing bottom-bounce interference (surface reflections for a receiving array). Choice of transducer geometry for a real system will depend on implementational details that are beyond the scope of the present work.

The receiver was assumed to be either an omni-directional hydrophone or a circular disk, as above.

Transmitter power was varied between 0.5 and 4 watts, subject to the constraint that the cavitation limit not be exceeded [14] for depths equal to the range. The signal suffered both spherical spreading and volume absorption [15] and, at the receiver, was further degraded by sea-state noise [14]. Operating frequencies between one and 100 kilohertz were considered although, for ranges of interest, optimal frequencies were found to be between 5 and 40 kHz.

Range was varied between 0.1 and 10 kilometers, although primary emphasis was placed on relatively short ranges between 1 and 4 km. Even deeper bottomed buoys can be made to operate within this range by attaching the transmitter to a subsurface float. As illustrated below, diversity techniques can substantially extend the operational range of systems tuned for such short range operation.

### 3.2 Fluctuations

The existence of time dependent amplitude fluctuations in underwater acoustic transmission is well documented. Urick attributes such behavior to the existence of temperature inhomogeneities which have been measured to have a scale length between 60 and 500 centimeters [14]. The resulting refractive index variations produce multipathing, and subsequent amplitude and phase variations at the receiver due to interference effects. Turbulence and water currents cause these effects to vary with time, and hence should have greatest impact at relatively shallow depths.

Whitmarsh and Leiss [16] have measured 20 to 30 dB fluctuations over a one minute interval in both horizontal and vertical (slant range) experiments. In the slant range measurements, fluctuations were observed to increase as the transmitter depth increased and the system assumed a more nearly vertical geometry. Whitmarsh [17] reports Rayleigh amplitude distributions in at-sea pulse experiments that include a surface reflection transmission path. These results are illustrated in Figures 3 and 4, respectively. Stone and Mintzer [18] have observed similar fluctuations in laboratory experiments. As noted above, digital transmission experiments have been limited by time dependent fluctuations.

In the present study, time dependent fluctuations are modeled as Rayleigh fading. This model is intuitively pleasing since Rayleigh fading is obtained if the

received signal is the vector sum of sine waves whose phase changes slowly (relative to the bit rate) with time [19], and thus can be represented as a random Gaussian process. The vector sum signal then has an envelope that changes with time and is Rayleigh distributed. This model is routinely used to describe fading in RF communications channels.

### 3.3 Modulation

In light of the time dependent fluctuations observed previously, a modulation scheme that is particularly robust to fading was chosen for the present study [20]. Frequency Shift Key (FSK) modulation simply transmits sinusoidal signals at two different frequencies corresponding to the binary symbols 1 and 0 respectively. Both frequencies should be large relative to the data rate so that many cycles are transmitted for each symbol. Figure 5 represents schematically a noncoherent FSK detector, consisting of bandpass filters for the two frequencies, envelope detectors, and a comparator [20]. A zero or a one is recorded by subtracting the output of the two envelope detectors and examining the sign of the difference. Thus the difference signal is compared to zero volts, independent of the amplitude variations of the received FSK signals due to fading.

By contrast to FSK, the decision threshold level for a simpler modulation scheme, Amplitude Shift Key (ASK), depends on the amplitude of the received signal. This results in very poor performance in a fading environment.

The probability of any given bit being in error as a function of gamma, the energy per bit divided by the noise spectral density (closely related to the SNR), is given by the equations shown in Figure 6 [19]. Implicit in this description is an assumption of white Gaussian noise, requiring pre-whitening filters. Additional spectrum shaping may be required to equalize the upper and lower sidebands of the FSK signal, since volume absorption is frequency dependent. Salz and Werner [21] demonstrated that this can be accomplished simply, requiring only the modulation of the amplitude of the FM signal in unison with the frequency. These implementational details will be assumed in the following discussion.

The probability of successful transmission increases exponentially with SNR in a nonfading environment; with

fading, only a linear increase is obtained. Alternatively, Figure 6 shows that the probability of error falls off exponentially with increasing signal-to-noise ratio in the absence of fading, but only as the reciprocal of the SNR in a fading environment. This behavior is illustrated in Figure 7 [19], where nonfading coherent FSK performance is also plotted. The harmful effect of fading is readily apparent. To achieve a given error probability, $10^{-5}$ for example, requires a 36 dB improvement in SNR corresponding to increasing transmitter power by about a factor of 4096, an unacceptable solution given sonobuoy constraints on cost and volume.

Obviously, fading, if present, is the dominant factor in reliable digital acoustic transmission, even for a robust modulation scheme like FSK. The measurements cited above strongly suggest that fading may be a serious problem. More specifically, Figure 8 shows data taken from Quazi, et al. [13], along with theoretical predictions. The solid curve represents 2-phase PSK (Phase Shift Key) transmission without fading while the dashed curve shows predicted performance with fading. Clearly the data are much closer to the fading curve and reinforce the assertion that fading must be considered in designing an underwater digital acoustic data-link.

### 3.4 Diversity

Since data suggest that fading is an important consideration in an underwater digital acoustic link, and since the required increase in power to provide sufficient margin against fading is not feasible for a sonobuoy system, alternative strategies must be employed. A common technique to overcome a fading communications channel in the telecommunication industry is diversity [22], that is, the use of statistically independent redundant channels. The application of diversity to the sonobuoy environment is discussed below.

Because the deleterious effects of fading are due to the tail of the amplitude probability distribution, merely increasing the mean of the distribution, by increasing transmitted power, is not an efficient method for providing the orders of magnitude performance improvement desired. However, combining signals transmitted on independent diversity channels results in a final probability distribution that goes as the product of the independent distributions. In other words, the probability of all channels fading

simultaneously is small relative to the probability of fading for a single channel.

A number of techniques are used to combine diversity channel signals. The simplest of these, selection combining, merely selects the branch with the largest signal-to-noise ratio. In practice, the branch with the largest (S + N) is usually used, since it is difficult to measure SNR dynamically. Considerably more sophisticated, and providing superior performance, is maximal ratio combining. In this method, first proposed by Kahn [23], the signals are weighted proportionately to their signal voltage to noise ratios, cophased, and summed coherently. Both selection combining and maximal ratio combining are considered below.

In order to employ diversity techniques, independent transmission channels must be available. In the sonobuoy case, frequency diversity, that is, simultaneous transmission of the same data at two or more frequencies, is the obvious solution. If sufficient power is available at the transmitter, frequency diversity appears to be feasible for implementation.

Alternatively, consider the situation illustrated in Figure 9, where multiple receiver buoys have been deployed within the main beam of the transmitter. If the transmitter depth is 3 kilometers and the transmitter beam is 30 degrees wide, the projection on the surface is a circle with a diameter of 1.6 kilometers. Separation of the receivers by many times the scale length of the underlying refractive index variation (about 500 centimeters) should result in statistically independent transmission paths, as required for diversity combining. Even if there is significant residual correlation between the diversity branches, Jakes [24] (and references therein) demonstrate that substantial improvement is obtained relative to the single branch performance.

This alternative type of diversity is termed spatial diversity. The principal advantage of spatial diversity is that no increased power is required at the transmitter. Simple receiver buoys, each radioing the received signal to the aircraft, can be employed, and combining can be performed on the aircraft. If deployment scenarios preclude the use of multiple buoys, use of a vertical array of widely separated independent receivers may also be possible.

Figure 10 shows the predicted performance for noncoherent FSK with diversity [19]. Note that, as anticipated, for large SNRs the diversity performance simply scales as the product of the diversity channels. The predicted behavior is plotted in Figure 11, along with the no-fading performance (dashed curve). Even for a probability of error of $10^{-5}$, nonfading performance is essentially recovered with a diversity of four. For completeness, the analogous equations for coherent FSK and selection combining are presented in Figure 12.

### 3.5 MSK Modulation

In the discussion of the Shannon channel capacity limit for a noisy communications channel, it was observed that the payoff was great for optimal bandwidth utilization, since channel capacity depends linearly on bandwidth and only logarithmically on signal power. Sinnema notes that for a deviation ratio (h) of one half (the ratio of the 0-1 frequency difference to the data rate) FSK transmission requires a bandwidth of 2.5 times the data rate [12]. Minimum Shift Key (MSK) modulation, a variation of FSK, transmits 99% of the mean power for an $h = 1/2$ signal in a bandwidth only 1.17 times the data rate [25]. Equivalently, MSK can transmit at about twice the data rate of FSK in a given bandwidth channel, while providing similar error performance. It is for this reason $h = 1/2$ MSK is sometimes referred to as fast FSK (FFSK) [26].

Figure 13 provides a mathematical description of MSK modulation [27]. The important difference between FSK and MSK is that in MSK modulation the phase is, at all points, including transitions between bits, a continuous function of time. This results in a very compact spectrum, as illustrated in Figure 14, where the power spectrum and the fraction of out of band power for MSK modulation are displayed [28]. Also shown in this figure are the equivalent curves for Phase Shift Key (PSK) modulation, a scheme previously used for an underwater data-link [13]. Note the much slower fall-off for the PSK signal; it has not reached 99% (-20 dB) power containment in the frequency spread of the figure.

In other respects, including a zero-volt threshold level independent of amplitude, MSK is quite similar to FSK. Because of its effective bandwidth utilization, MSK will be considered along with FSK in the following discussions of a digital link for sonobuoys.

Figures 15 through 17 show the MSK probability of error in channels with and without fading, and for both selection combining and maximal ratio combining [29] [30]. At large SNRs both selection combining and maximal ratio combining display the same functional dependence on gamma. There is, however, a significant difference in the associated multiplicative coefficients. For 4-fold diversity (M = 4) the selection combining coefficient is 105/32 while that for maximal ratio combining is 35/256. This results in the probability of error for selection combining being 24 times larger than for maximal ratio combining.

## 4. RESULTS

### 4.1 An Optimum System

First, consider an optimal, although unrealizable, system. The transmitter consists of a piston radiator with a 30 degree beamwidth (or any other desired angle) between 3 dB points, independent of frequency, but subject to a constraint on maximum transducer diameter of 10 or 15 centimeters, roughly corresponding to A or B sized sonobuoy canisters. Frequency will vary to produce the optimum SNR at each range considered, and the transmitter size will vary appropriately to maintain a constant DI (directivity index), subject to the maximum diameter constraint.

Although initially appearing somewhat arbitrary, this parameterization of the transmitter is based on the belief that the accuracy with which receiver buoys can be located relative to the transmitter, will set an upper limit on useful DI. Thus, keeping the beam pattern constant over frequency is just a reflection of finite positioning accuracy. The limit on maximum transducer diameter stems from the standardized size of sonobuoy containers and launch tubes.

The receiver is assumed to be either an omni-directional hydrophone or to be identical to the transmitter. All calculations assume sea state 6, and in this section, the radiated power is 0.5 watts. Range is varied from 0.1 to 10 kilometers. A 2340 Hz bandwidth is employed.

First, at a 3 kilometer range, SNR is calculated as a function of frequency for a system with an omni-directional receiver and a transmitter diameter of 15 centimeters. The results are shown in Figure 18. The relevant feature to note is the peak in the curve,

indicating that at this range there is a well-defined frequency producing an optimum SNR.

Similar results are obtained over all ranges of interest. The frequency that optimizes SNR is plotted in Figure 19, as a function of range. At short range, very high frequencies produce optimum performance, although the optimum frequency falls rapidly due to the strong frequency dependence of volume absorption. At approximately one km the optimum frequency levels off at 19.67 kHz and remains constant through about 2.3 km. Up to this point the transmitter diameter had been increasing continuously to maintain constant DI as the frequency fell. Near one km the maximum diameter, 15 cm, was reached. Beyond this point, DI falls with lower frequency since the diameter is fixed. Therefore, in the region between 1.0 and 2.3 km the optimum frequency is constant, maintaining the DI. Beyond 2.3 km this effect is overwhelmed by volume absorption, and the frequency falls again. The SNR obtained with optimum frequencies is plotted in Figure 20. These curves, while not describing any single system, allow the acoustic-link designer to select an optimum frequency for the range of interest, to estimate SNR at that range, and to note the sensitivity of the optimum frequency and SNR to range variations.

Normally, at this point in the design of an acoustic link, fixed values for frequency and transmitter size would be specified, and performance prediction made for a realizable system. However, in order to acquire some familiarity with optimal system performance, the optimum frequencies will be retained for some performance predictions. The next section will specialize to some realistic systems.

The solid curve in Figure 21 shows the Shannon limit on channel capacity, calculated for the optimum system. With optimum coding, using the maximum number of destinguishable signal levels that a channel of fixed transmitter power and noise level can accommodate, this channel theoretically can support data rates in excess of 10 kilobits/s to a range of about 6.8 kilometers and 5 kilobits/s to ranges beyond 10 kilometers. Using the criteria that the signal-to-noise ratio should be reduced by a factor of 1/7 to predict realistic system performance, the dashed curve is obtained. Then, the 10 kilobit/s range is reduced to 4 kilometers, and at 10 kilometers, only 1 kilobit/s data rates can be maintained.

Specializing to (sub-optimum) FSK coding however, a channel of this bandwidth can support only a 936 bit/s data rate. Since, as shown in Figure 7, there is only a small performance difference at high signal-to-noise ratios between coherent and noncoherent FSK, noncoherent detection will be assumed for the remainder of this section. Then, using the equations from Figure 10, and the optimum SNRs from Figure 20, the probability of error as a function of range can be calculated under various fading and diversity assumptions. These calculations are plotted in Figure 22. The solid curve on the right side of the figure shows optimal performance in a nonfading environment, while the solid curve to the left and above is for the same system in a fading channel. The three dashed curves illustrate the striking improvement afforded by diversity. From left to right, these curves correspond to 2, 4, and 8 diversity branches respectively. For a target probability of error of $10^{-3}$ , the maximum range at which this system is operational is 8.1 km without fading, 0.8 km with fading and no diversity, and 3.6, 7.0, and 9.8 km for the three diversity options considered.

A similar calculation for MSK, with maximal ratio combining for the diversity cases, is shown in Figure 23. Note that with MSK modulation, the same channel can now support 2000 bit/s transmission. At $10^{-3}$ probability of error, nonfading and fading channels without diversity are essentially identical to the FSK case. Because maximal ratio combining was assumed, the diversity performance is somewhat better than for FSK.

In these, and all subsequent calculations, no margin was allowed for sub-optimum alignment between the transmitter and the receiver. Calculations in the following section however, do vary transmitter power. The effect of misalignment can be seen there by simply reducing the power an appropriate amount.

Finally, consider the effect of employing a directional receiver, identical to the transmitter. Figure 24 shows the result of an optimum frequency calculation for this system. The main effect is the lengthening of the 19.67 kHz plateau, extending it to about 3.5 km. Similar behavior is obtained for 10 centimeter transducers, but with a narrower plateau at a frequency of 29.5 kHz.

## 4.2 A Realizable System

Now, focus on realizable systems where transmitter size and frequency are fixed. Transmitter diameters of 10 and 15 centimeters are considered, operating at the plateau frequencies 29.5 kHz and 19.67 kHz respectively. This parameter choice yields beam patterns that are 30 degrees between -3 dB points. Transmitter powers of 0.5, 1, 2, and 4 watts are employed with omni-directional receivers. Channel bandwidths are varied to produce FSK data rates of 438, 936, and 2000 bits/s and MSK data rates of 936, 2000, and 4274 bits/s. Sea-state 6 noise is assumed in all cases.

A sample calculation for a 15 centimeter transmitter operating at 0.5 watts and an omni-directional receiver is shown in Figure 25. This figure is directly comparable to Figure 22, both in format and in parameter choice, except for the current requirement of fixed transmitter size and frequency. For the realistic system, the envelope of the curves is much narrower, and is shifted to substantially shorter range. This is characteristic of all calculations in this section relative to the optimal systems discussed previously.

At this point, consider the "brute force" alternative to diversity in a fading channel; simply increasing transmitter power to provide the requisite margin. Figure 26 shows the power required to provide a $10^{-3}$ probability of error, with the current system, as a function of range. The infeasibility of this approach is evident, with an increase in power from 1 to 1000 watts only providing a corresponding increase in range from 1.1 to 5.1 kilometers.

Figures 27 and 28 show identical calculations for a 10 cm transmitter operating at 29.5 kHz. Note the still tighter bunching of the curves at short range, and the still greater inability of increased transmitter power to extend the reliable transmission range.

Tables 1 and 2 summarize performance (for omni and directional receivers respectively) of 0.5 watt systems; both optimal and realistic systems are considered. Values above the solid line are the range at which a $10^{-3}$ probability of error is obtained with 15 centimeter transducers; values below correspond to 10 centimeter transducers. Tables 3 through 6 show the range for a $10^{-3}$ probability of error and the full range of parameter choices discussed at the beginning of this section.

### 4.3 A Commercial System

A relatively low data rate (80 bits/s) commercial product embodying many of the ideas discussed above has recently been introduced by Oceano Instruments U.S.A., Inc. [31]. The DT 122 Acoustic Data Transmission System is a bi-directional digital communications system for target markets including telemetry links for RCVs (Remotely Controlled Vehicles) and monitoring and control of underwater oil exploration and recovery equipment.

The system is made up of an identical pair of DT 122 units that are able to send and receive data. A binary message, generated outside the system, is translated into a secure, error-detecting code, and acoustically transmitted by the first DT 122. On message reception, the second DT 122 translates this message back into binary code.

Figure 29 shows some of the relevant operating parameters for the DT 122 system. Operating at frequencies near 20 kHz and at a peak power of 375 watts applied to the transmitter, the DT 122 system functions within the range of parameters estimated for nondiversity transmission.

## 5. CONCLUSIONS AND RECOMMENDATIONS

Although somewhat cursory, this study does indicate that a low power, digital acoustic-link is feasible for underwater communications. Data rates up to a few kilobits per second, and ranges of several kilometers appear well within the limits of current technology. Of course, the model employed could be refined in various places; for example, the assumed pre-whitening and spectrum shaping could be quantified and included in the calculation. Without some guidance from measurements however, it is difficult to know where additional effort would be profitable. The primary recommendation is therefore, to measure the performance of a digital link whose parameters and geometry are chosen with regard to a specific application. In particular, since the assumption of fading dominates all performance predictions, the presence and severity of fading must be verified. Indeed the counter-intuitive results obtained from the slant-range measurements discussed above (fluctuations increasing with increasing transmitter depth) highlight the need for experimental data. Additionally, the feasibility of the proposed spatial

diversity implementation also requires experimental validation. While the scattered data cited above provide a superficial indication, they are not an adequate substitute for a coherent set of measurements.

*References*

1. Rowlands, R. O. and Quinn, F. G., "Transmission Rate Limits in Underwater Acoustic Telemetry", "Underwater Acoustics, Volume 2", V. M. Albers, editor, Plenum Press, 393, (1967)

2. le Blanc, L. R., "Channel Capacity of the Underwater Acoustic Data Link", Proceedings of the National Telecommunications Conference, 262 (1967)

3. Rowlands, R. O. and Quinn, F. G.,"The Spacing of Underwater Arrays for a Diversity Reception Acoustic Telemetering System", Proceedings of the National Telecommunications Conference, 266, (1967)

4. Konrad,W. L., "A Long Range Speech Transmission Experiment", Proceedings of the National Telecommunications Conference, 325, (1967)

5. Smith, C. E., "An Underwater Communications System for Deep Submergency Applications", Proceedings of the National Telecommunications Conference, 328, (1967)

6. Painter, D. W., "Deep Vehicle Telemetry", Proceedings of the National Telecommunications Conference, 342, (1967)

7. Andrews, G., "Acoustic Telemetering for Sea-State Six Operations", Proceedings of the National Telecommunications Conference, 351, (1967)

8. Tarasyuk, Y. F., "Transmission of Information Underwater", Peredacha Informatsii pod Vodoi, Moscow, (1974)

9. Tarasyuk,Y. F. and Seravin, G. N., "Hydroacoustic Telemetry", Gidroakusticheskaya Telemetriya, Leningrad, (1973)

10. Shannon, C. E., "A Mathematical Theory of Communications", BSTJ, Vol. 27, 379-623, (1948)

11. Shannon, C. E., "Communication in the Presence of Noise", Proc. IRE, Vol. 37, 10, (1949)

12. Sinnema, W., "Digital, Analog, and Data Communication", Reston Publishing Company, Inc., (1982)

13. Quazi,A. H., Lackoff, M. R., Viccione, D. M., Gannon, E. C. and Kurth, R. R., "High Data Rate Acoustic Communications: Experimental Results (U)", Journal of Underwater Acoustics, Vol. 27, 653, (1977) (CONFIDENTIAL)

14. Urick, R. J., "Principals of Underwater Sound, Second Edition", McGraw Hill, Inc., (1975)

15. Urick, R. J., "Sound Propogation in the Sea", Peninsula Publishing, (1982)

16. Whitmarsh, D. C. and Leiss, W. J., "Fluctuation in Horizontal Acoustic Propagation over Short Depth Increments", JASA, Vol. 43, 1036, (1968)

17. Whitmarsh, D. C., "Underwater-Acoustic-Transmission Measurements", JASA, Vol. 35, 2014, (1963)

18. Stone, R. G. and Mintzer, D., "Range Dependence of Acoustic Fluctuations in a Randomly Inhomogeneous Medium", JASA, Vol. 34, 647, (1962)

19. Whalen, A. D., "Detection of Signals in Noise", Academic Press, (1971)

20. Carlson, A. B., "Communication Systems", McGraw Hill, Inc., (1968)

21. Salz, J. and Werner, J. J., "Spectral Shaping by Simultaneous Amplitude and Frequency Modulation", BSTJ, Vol. 59, 557, (1980)

22. "Transmission Systems for Communications", Bell Telephone Laboratories, Inc., (1982)

23. Kahn, L. R., "Ratio Squarer", Proc. IRE (Corresp.), Vol. 42, 1704, (1954)

24. Jakes, W. R., editor, "Microwave Mobile Communications", John Wiley & Sons, (1974)

25. Prabhu, V. K., "Spectral Occupancy of Digital Angle-Modulation Signals", BSTJ, Vol. 55, 429, (1976)

26. de Buda, R. "Coherent Demodulation of Frequency Shift Keying With Low Deviation Ratio", IEEE Trans. on Communications, Vol. COM-20, 429, (1972)

27. Haykin,S. "Communications Systems", John Wiley & Sons, (1978)

28. Bellamy,J. "Digital Telephony", John Wiley & Sons, (1982)

29. Schwartz, M., Bennett, W. R. and Stein, S., "Communication Systems and Techniques", McGraw Hill, Inc., (1966)

30. Sundberg, C. -E., "Error probability of Partial Response Continuous-Phase Modulation with Coherent MSK-Type Receiver, Diversity, and Slow Rayleigh Fading in Gaussian Noise", BSTJ, Vol. 61, 1933, (1982)

31. Oceano Instruments, U.S.A., Inc., P. O. Box 55489, Seattle, Washington 98036, (206)-774-7226

**TABLE 1.** RANGE (km) FOR $10^{-3}$ BER

OMNI Receiver

| System* | Mod | Diversity 1 | 2 | 4 | 8 |
|---|---|---|---|---|---|
| OPT | FSK | 0.8 | 3.6 | 7.0 | 9.8 |
| REAL | FSK | 0.8 | 3.4 | 5.3 | 6.5 |
| OPT | MSK | 0.8 | 3.9 | 7.8 | *** |
| REAL | MSK | 0.8 | 3.6 | 5.7 | 7.0 |
| OPT | FSK | 0.8 | 3.0 | 5.7 | 8.1 |
| REAL | FSK | 0.8 | 2.4 | 3.4 | 4.1 |
| OPT | MSK | 0.8 | 3.2 | 6.4 | 9.3 |
| REAL | MSK | 0.8 | 2.5 | 3.7 | 4.3 |

* upper half 15 cm, lower half 10 cm directional transducers operating at 0.5 watts in a 2340 Hz channel (FSK modulation at 936 bits/s, MSK modulation at 2000 bits/s)

*** denotes range beyond the limit (10 km) of the curves from which this data was obtained

**TABLE 2.** RANGE (km) FOR $10^{-3}$ BER

Directional Receiver

| System* | Mod | Diversity 1 | 2 | 4 | 8 |
|---|---|---|---|---|---|
| OPT | FSK | 2.4 | 7.0 | *** | *** |
| REAL | FSK | 2.4 | 6.2 | 8.3 | 9.6 |
| OPT | MSK | 2.4 | 7.4 | *** | *** |
| REAL | MSK | 2.4 | 6.4 | 8.7 | *** |
| OPT | FSK | 1.9 | 5.1 | 8.4 | *** |
| REAL | FSK | 1.9 | 3.9 | 5.1 | 5.7 |
| OPT | MSK | 1.9 | 5.4 | 9.3 | *** |
| REAL | MSK | 1.9 | 4.0 | 5.3 | 6.0 |

* upper half 15 cm, lower half 10 cm directional transducers operating at 0.5 watts in a 2340 Hz channel (FSK modulation at 936 bits/s, MSK modulation at 2000 bits/s)

*** denotes range beyond the limit (10 km) of the curves from which this data was obtained

**TABLE 3.** RANGE (km) for $10^{-5}$ BER

- Noncoherent FSK
- 19.67 kHz
- 15 cm transmitter, omni-directional receiver

| | | Power (watts) | | | |
|---|---|---|---|---|---|
| Rate | M | 0.5 | 1 | 2 | 4 |
| 438 | 1 | 1.2 | 1.4 | 1.7 | 2.1 |
| 936 | 1 | 0.8 | 1.1 | 1.3 | 1.7 |
| 2000 | 1 | 0.6 | 0.8 | 1.1 | 1.3 |
| 438 | 2 | 4.0 | 4.5 | 5.0 | 5.5 |
| 936 | 2 | 3.4 | 3.9 | 4.4 | 4.9 |
| 2000 | 2 | 3.0 | 3.4 | 3.8 | 4.4 |
| 438 | 4 | 5.9 | 6.5 | 7.1 | 7.6 |
| 936 | 4 | 5.3 | 5.8 | 6.4 | 7.0 |
| 2000 | 4 | 4.7 | 5.3 | 5.7 | 6.4 |
| 438 | 8 | 7.1 | 7.6 | 8.3 | 8.8 |
| 936 | 8 | 6.5 | 7.0 | 7.6 | 8.2 |
| 2000 | 8 | 5.8 | 6.4 | 7.0 | 7.6 |

**TABLE 4.** RANGE (km) for $10^{-3}$ BER

- MSK - Maximal Ratio Combining
- 19.67 kHz
- 15 cm transmitter, omni-directional receiver

| | | Power (watts) | | | |
|---|---|---|---|---|---|
| Rate | M | 0.5 | 1 | 2 | 4 |
| 936 | 1 | 1.1 | 1.4 | 1.7 | 2.0 |
| 2000 | 1 | 0.8 | 1.1 | 1.3 | 1.6 |
| 4274 | 1 | 0.6 | 0.8 | 1.0 | 1.3 |
| 936 | 2 | 4.2 | 4.7 | 5.2 | 5.7 |
| 2000 | 2 | 3.6 | 4.1 | 4.6 | 5.2 |
| 4274 | 2 | 3.2 | 3.6 | 4.1 | 4.6 |
| 936 | 4 | 6.3 | 6.8 | 7.4 | 8.0 |
| 2000 | 4 | 5.6 | 6.3 | 6.8 | 7.3 |
| 4274 | 4 | 5.1 | 5.6 | 6.2 | 6.7 |
| 936 | 8 | 7.6 | 8.2 | 8.7 | 9.4 |
| 2000 | 8 | 7.0 | 7.5 | 8.2 | 8.6 |
| 4274 | 8 | 6.3 | 6.9 | 7.5 | 8.1 |

**TABLE 5.** RANGE (km) for $10^{-5}$ BER

- Noncoherent FSK
- 29.5 kHz
- 10 cm transmitter, omni-directional receiver

| | | Power (watts) | | | |
|---|---|---|---|---|---|
| Rate | M | 0.5 | 1 | 2 | 4 |
| 438 | 1 | 1.0 | 1.2 | 1.4 | 1.6 |
| 936 | 1 | 0.8 | 1.0 | 1.2 | 1.4 |
| 2000 | 1 | 0.6 | 0.8 | 1.0 | 1.2 |
| 438 | 2 | 2.7 | 3.0 | 3.3 | 3.6 |
| 936 | 2 | 2.4 | 2.7 | 3.0 | 3.3 |
| 2000 | 2 | 2.2 | 2.4 | 2.7 | 3.0 |
| 438 | 4 | 3.8 | 4.1 | 4.4 | 4.7 |
| 936 | 4 | 3.4 | 3.7 | 4.1 | 4.3 |
| 2000 | 4 | 3.2 | 3.4 | 3.7 | 4.0 |
| 438 | 8 | 4.4 | 4.7 | 5.0 | 5.3 |
| 936 | 8 | 4.1 | 4.4 | 4.7 | 5.0 |
| 2000 | 8 | 3.7 | 4.1 | 4.4 | 4.6 |

**TABLE 6.** RANGE (km) for $10^{-3}$ BER

- MSK - Maximal Ratio Combining
- 29.5 kHz
- 10 cm transmitter, omni-directional receiver

| | | Power (watts) | | | |
|---|---|---|---|---|---|
| Rate | M | 0.5 | 1 | 2 | 4 |
| 936 | 1 | 1.0 | 1.2 | 1.4 | 1.6 |
| 2000 | 1 | 0.8 | 1.0 | 1.2 | 1.4 |
| 4274 | 1 | 0.6 | 0.8 | 1.0 | 1.2 |
| 936 | 2 | 2.8 | 3.1 | 3.3 | 3.7 |
| 2000 | 2 | 2.6 | 2.8 | 3.1 | 3.4 |
| 4274 | 2 | 2.3 | 2.5 | 2.8 | 3.1 |
| 936 | 4 | 4.0 | 4.3 | 4.6 | 4.9 |
| 2000 | 4 | 3.6 | 4.0 | 4.3 | 4.6 |
| 4274 | 4 | 3.3 | 3.6 | 3.9 | 4.3 |
| 936 | 8 | 4.6 | 5.0 | 5.3 | 5.6 |
| 2000 | 8 | 4.3 | 4.6 | 5.0 | 5.2 |
| 4274 | 8 | 4.0 | 4.3 | 4.6 | 4.9 |

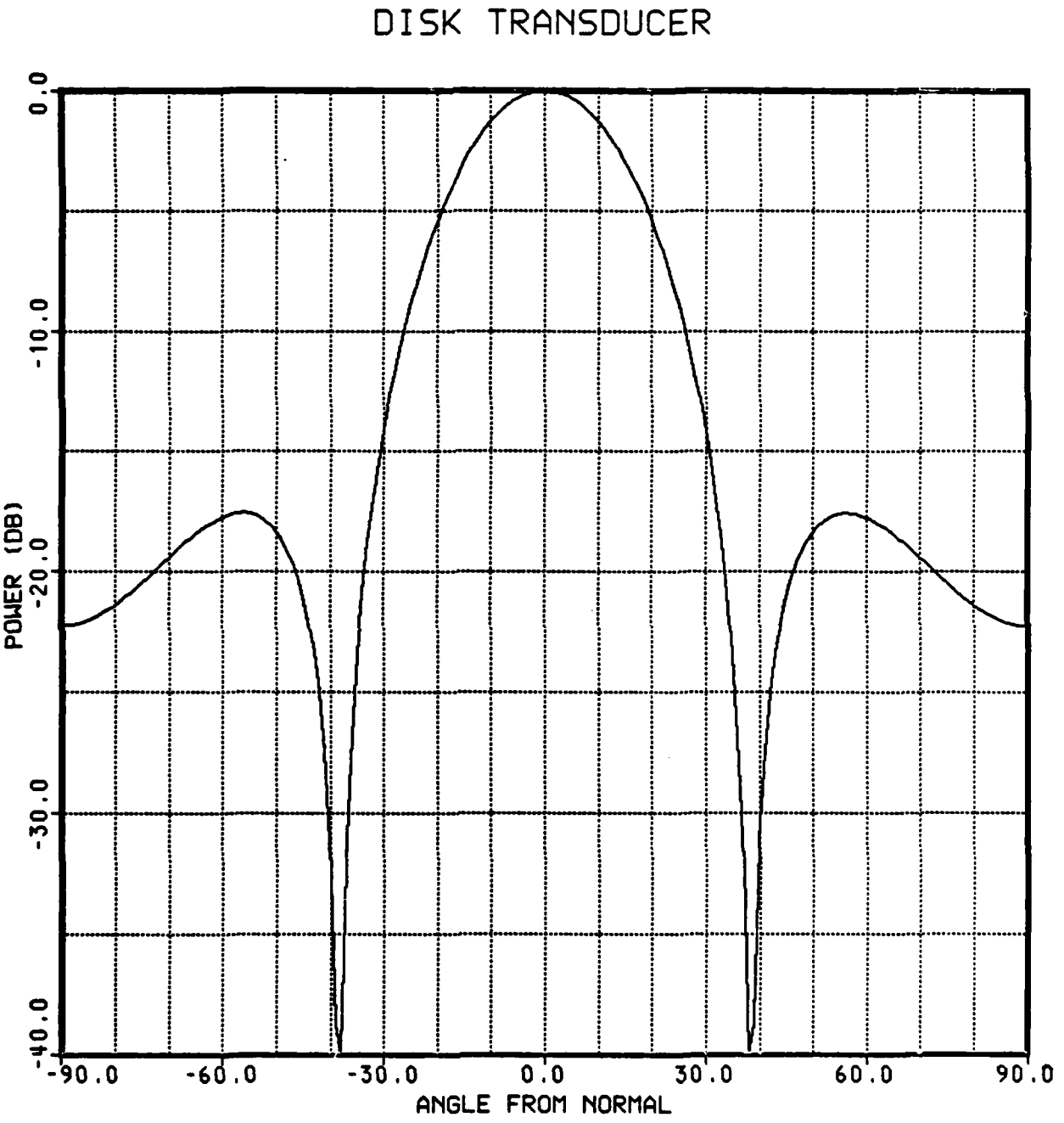


**Figure 1** Beam pattern for a circular piston radiator with 30 degrees between -3 dB points.

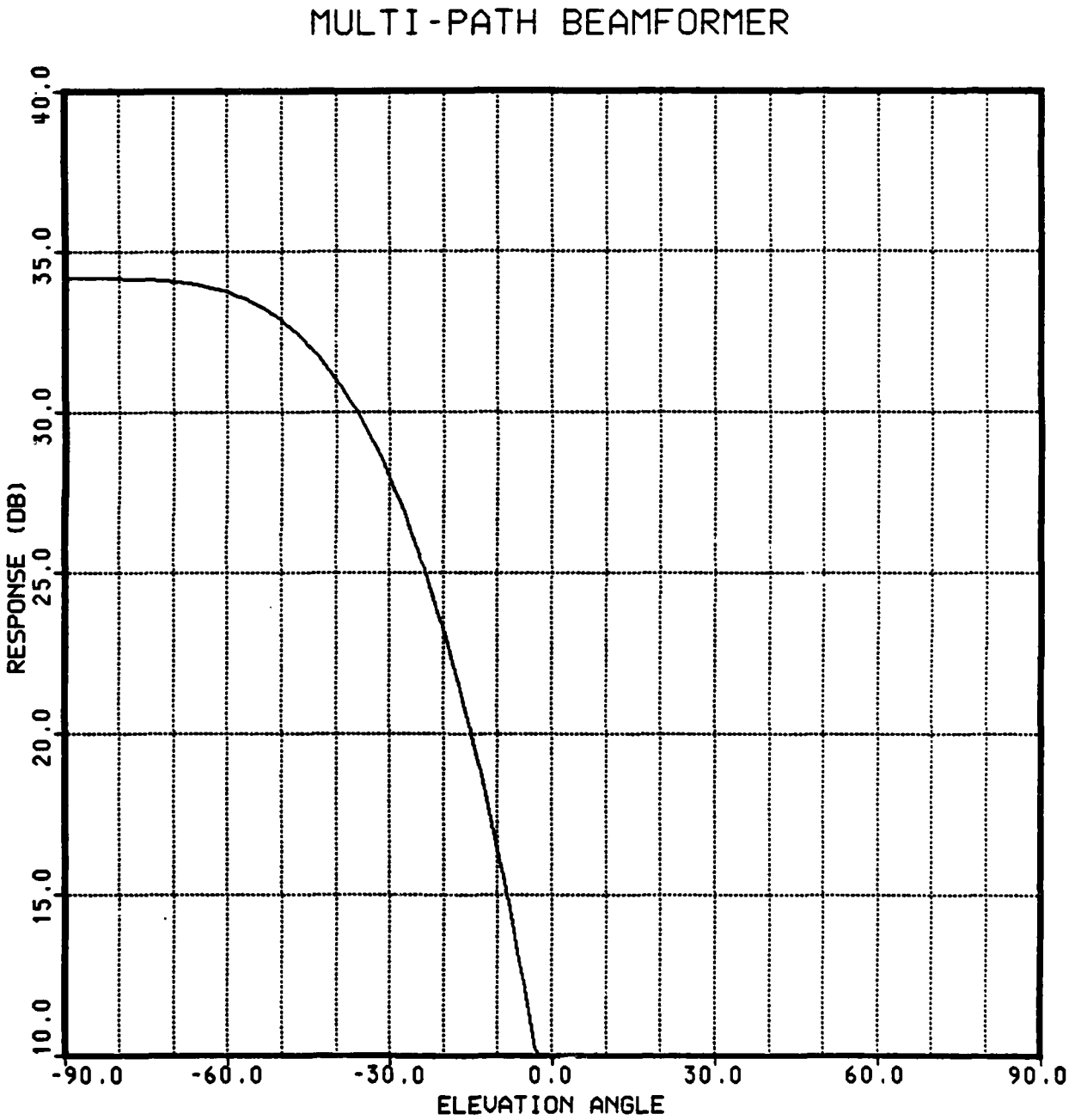


Figure 2 Beam pattern for a 10 element array with quarter wavelength spacing and binomial weighting.

# TIME DEPENDENT FLUCTUATIONS

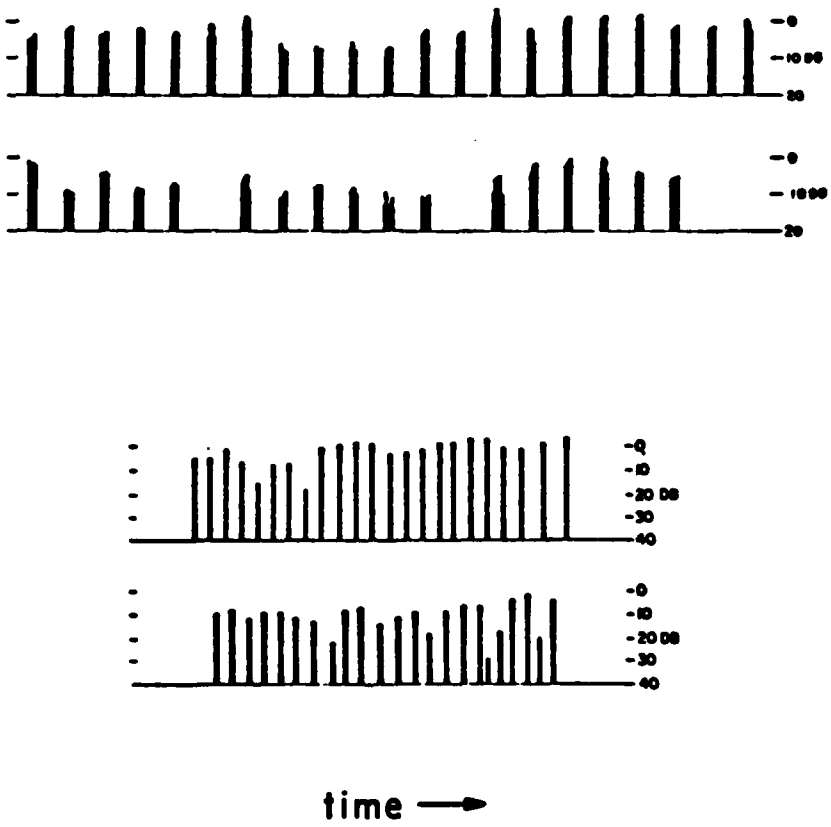


Figure 3 Amplitude variations from pulse experiments.

# RAYLEIGH AMPLITUDE DISTRIBUTIONS

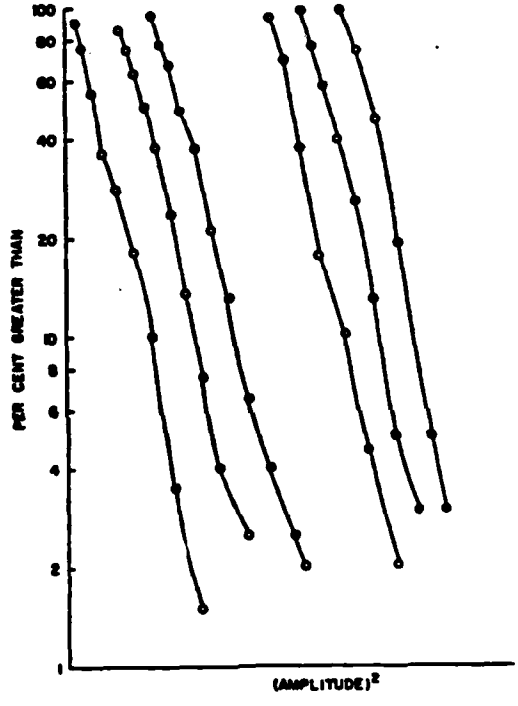


Figure 4 Rayleigh distribution of amplitudes from surface bounce pulse experiments. Individual curves are shown for different measurement geometries. A Rayleigh distribution produces a straight line on this axis system.

# NONCOHERENT FSK DETECTOR

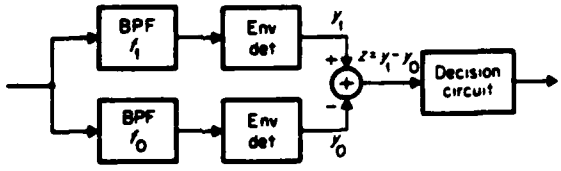


Figure 5 A noncoherent FSK detector.

# FSK AND RAYLEIGH FADING

PROBABILITY OF ERROR FOR:

- NO FADING

$$P_e = \tfrac{1}{2} e^{-\frac{\gamma}{2}}$$

- FADING

$$P_e = \frac{1}{2+\gamma}$$

$$\rightarrow \frac{1}{\gamma}$$

Figure 6 Error performance of noncoherent detection of FSK modulation with and without fading.

# FSK WITH FADING

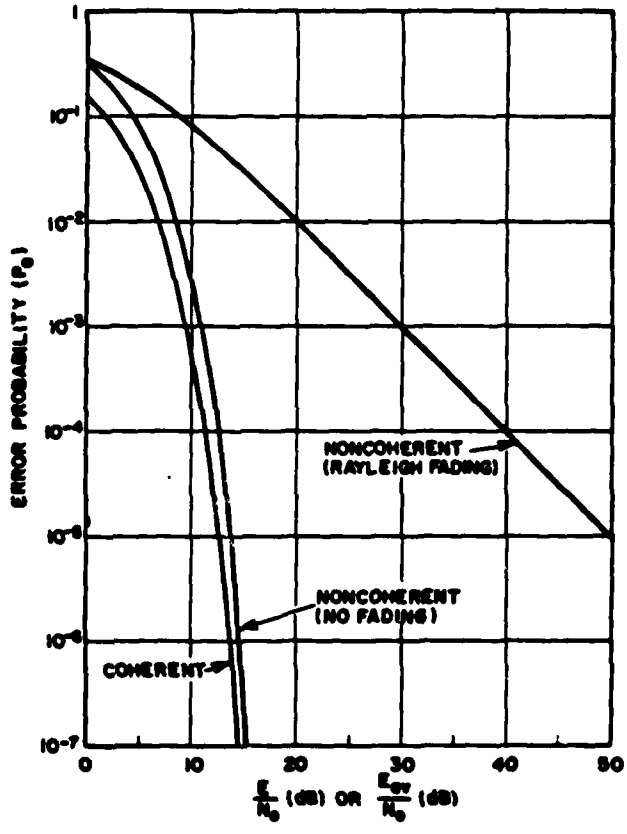


Figure 7 Error performance of FSK modulation with and without fading.

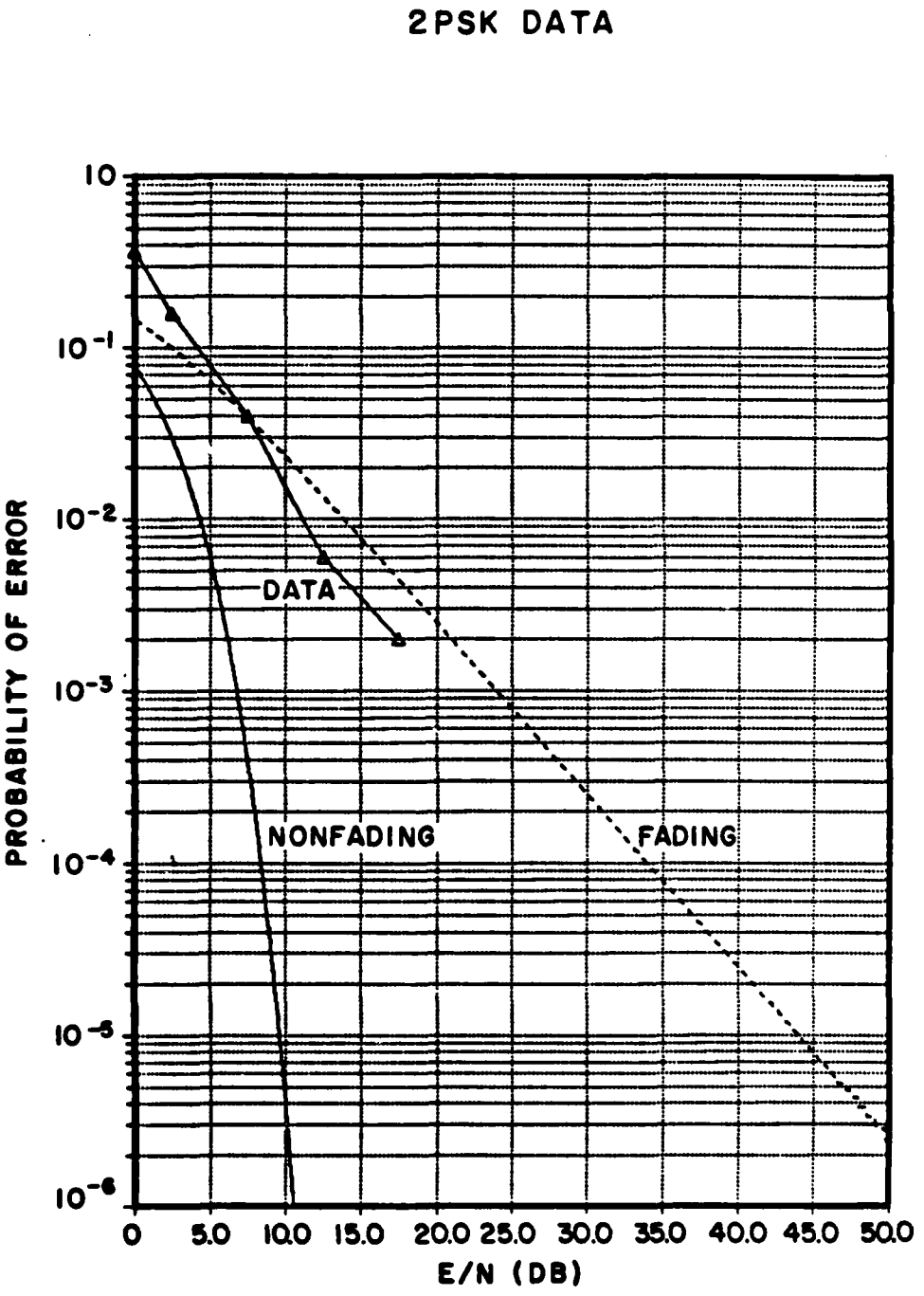


Figure 8 Measured error performance for an underwater digital acoustic-link with 2-PSK modulation. Data (triangles) are from Quazi et al. [13]. The solid curve represents 2-phase PSK (Phase Shift Key) transmission without fading while the dashed curve shows predicted performance with fading.

# DIVERSITY WITH SONOBUOYS

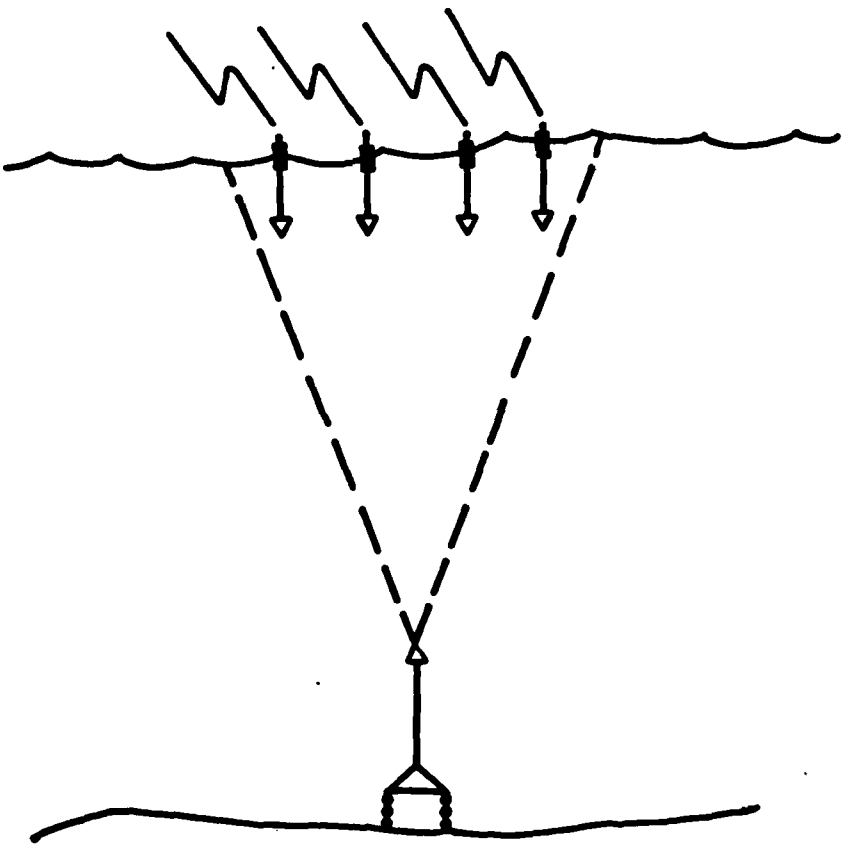

Figure 9 A possible implementation of spatial diversity with a sonobuoy acoustic link.

# NONCOHERENT FSK

PROBABILITY OF ERROR FOR:

- NO FADING - NO DIVERSITY

$$P_e = \tfrac{1}{2} e^{-\frac{\gamma}{2}}$$

- FADING - NO DIVERSITY

$$P_e = \frac{1}{2+\gamma}$$

$$\rightarrow \frac{1}{\gamma}$$

- FADING - M-fold DIVERSITY

$$P_e = \frac{1}{(2+\gamma)^M} \sum_{k=0}^{M-1} \binom{M+k-1}{k} \left(\frac{1+\gamma}{2+\gamma}\right)^k$$

$$\rightarrow \left(\frac{1}{\gamma}\right)^M$$

Figure 10 Equations for error performance of noncoherent detection of FSK modulation with diversity.

# NONCOHERENT FSK

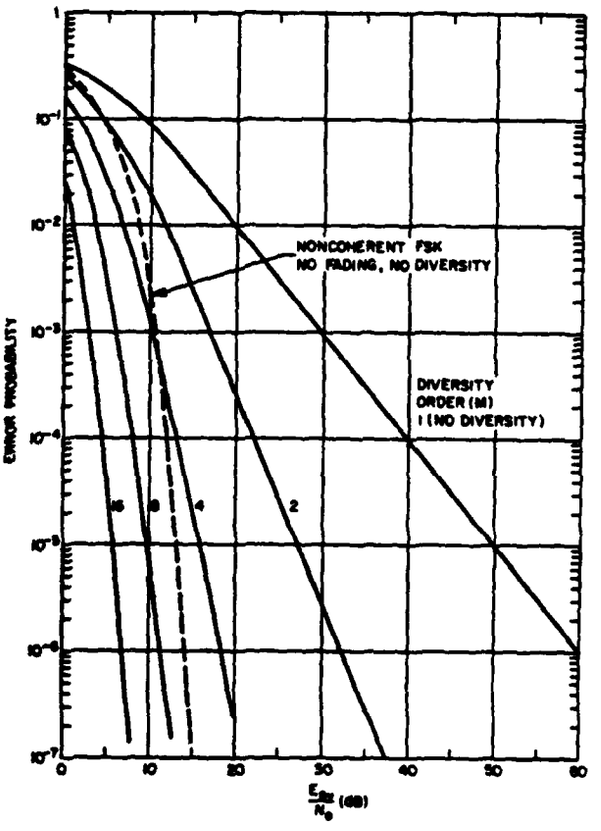


Figure 11 Graphs of error performance of noncoherent detection of FSK modulation with diversity.

# COHERENT FSK

PROBABILITY OF ERROR FOR:

- NO FADING - NO DIVERSITY

$$P_e = \tfrac{1}{2}\mathrm{erfc}\left(\sqrt{\gamma/2}\right)$$

- FADING - NO DIVERSITY

$$P_e = \frac{1}{2}\left[1 - \frac{1}{\sqrt{1+(2/\gamma)}}\right]$$

$$\rightarrow \frac{1}{2\gamma}$$

- FADING - M-fold DIVERSITY

$$P_e = \frac{1}{2}\sum_{j=0}^{M} \frac{(-1)^j \binom{M}{j}}{\sqrt{1+(2/\gamma)}}$$

$$\rightarrow \left(\frac{1}{\gamma}\right)^M$$

Figure 12 Equations for error performance of coherent detection of FSK modulation with diversity.

# MSK MODULATION

- MINIMUM SHIFT KEY MODULATION
- CONTINUOUS PHASE FSK

$$S(t) = A\cos[2\pi f_c t + \phi(t)]$$

$$S_1(t) = A\cos[2\pi f_1 t + \phi(0)]$$

$$S_0(t) = A\cos[2\pi f_0 t + \phi(0)]$$

$$\phi(t) = \phi(0) \pm \frac{\pi h}{T_b} t$$

$$= \phi(0) \pm \frac{\pi}{2T_b} t$$

- REQUIRED BANDWIDTH FOR $h = \frac{1}{2}$ MSK MODULATION IS $1.17 f_s$

Figure 13 A summary of MSK modulation.

# MSK POWER SPECTRUM

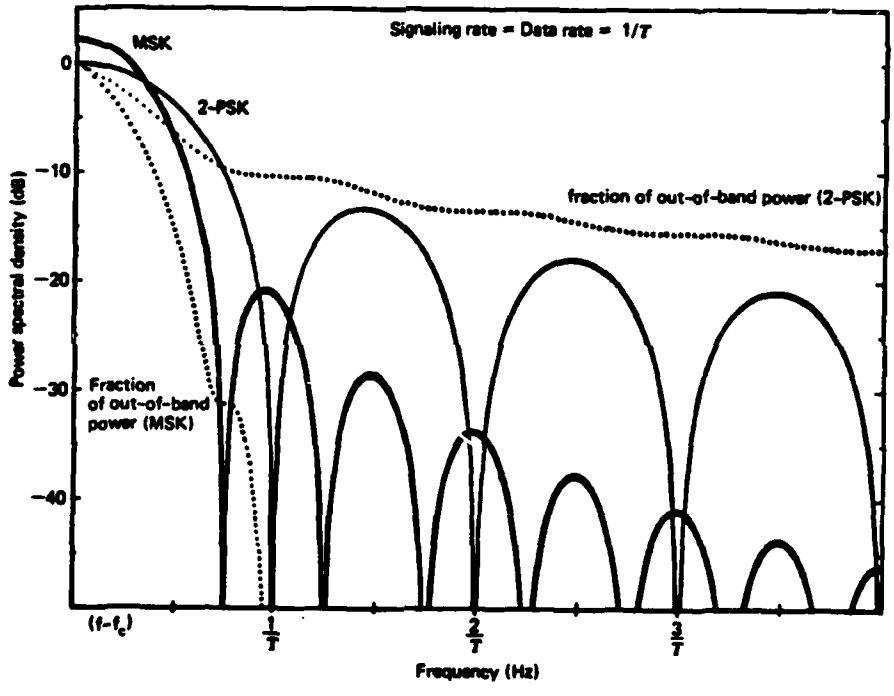


Figure 14 The power spectra of an MSK modulated signal and of a 2-PSK modulated signal.

# MSK

PROBABILITY OF ERROR $P_e = 2P_1 + P_1^2$

- NO FADING - NO DIVERSITY

  $P_1 = \frac{1}{2} erfc(\sqrt{\gamma})$

- FADING - NO DIVERSITY

  $$P_1 = \frac{1}{2}\left[1 - \frac{1}{\sqrt{1+(1/\gamma)}}\right]$$

  $$\rightarrow \frac{1}{4\gamma}$$

Figure 15 Equations for error performance of coherent detection of MSK modulation with and without fading.

## MSK cont.

- FADING - M-fold DIVERSITY
  - SELECTION COMBINING

$$P_1 = \frac{1}{2} \sum_{j=0}^{M} \frac{(-1)^j \binom{M}{j}}{\sqrt{1+(j/\gamma)}}$$

$$\rightarrow \left(\frac{1}{\gamma}\right)^M$$

Figure 16 Equations for error performance of coherent detection of MSK modulation with selection combining of diversity branches.

# MSK cont.

- FADING - M-fold DIVERSITY
  - MAXIMAL RATIO COMBINING

$$P_1 = \frac{1}{2}\left\{1 - \sqrt{\frac{\gamma}{1+\gamma}}\left[\sum_{j=0}^{M-1} \frac{\prod_{k=0}^{j}|2k-1|}{j!\ 2^j}(1+\gamma)^{-j}\right]\right\}$$

$$\rightarrow \left(\frac{1}{\gamma}\right)^M$$

Figure 17 Equations for error performance of coherent detection of MSK modulation with maximal ratio combining of diversity branches.

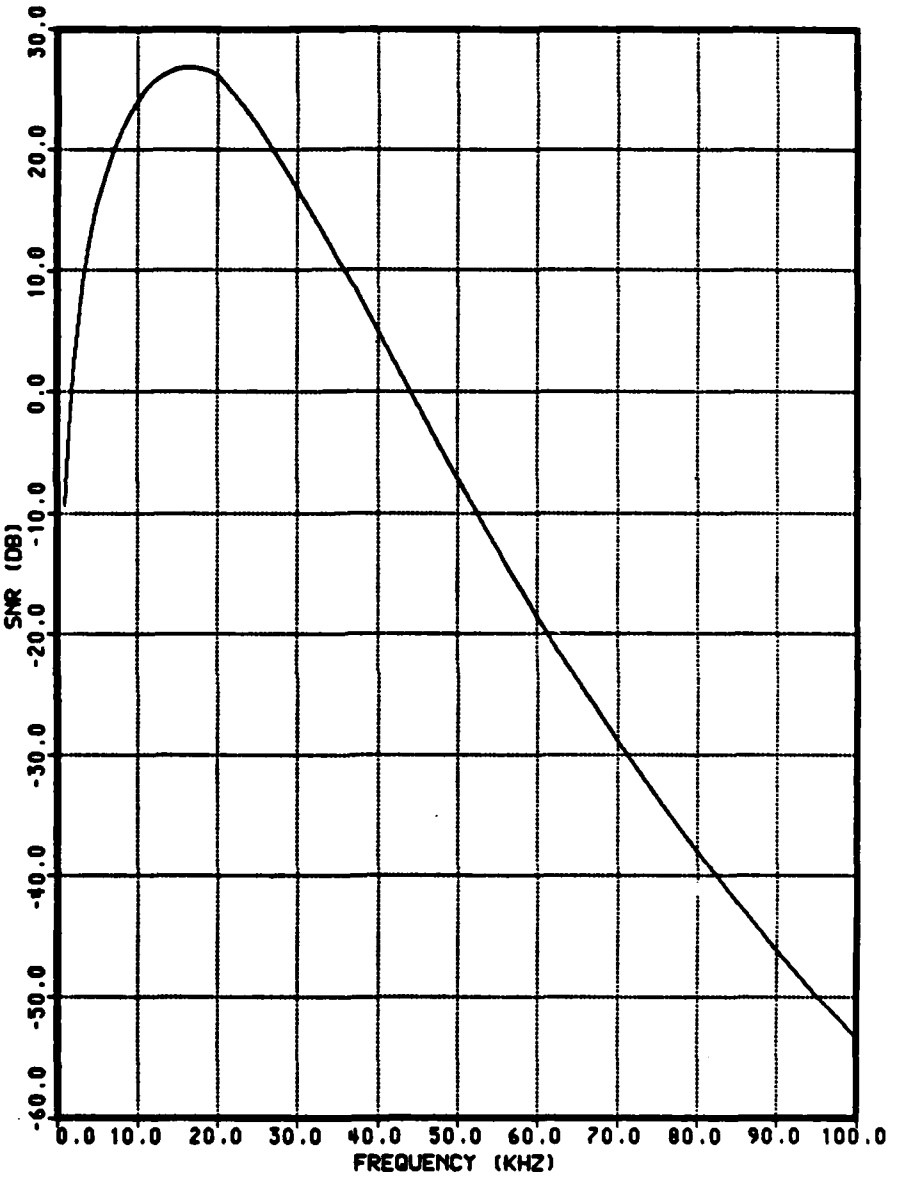


Figure 18 SNR as a function of frequency for a 0.5 watt link composed of a 15 cm transmitter and an omni-directional receiver operating at a 3 km range.

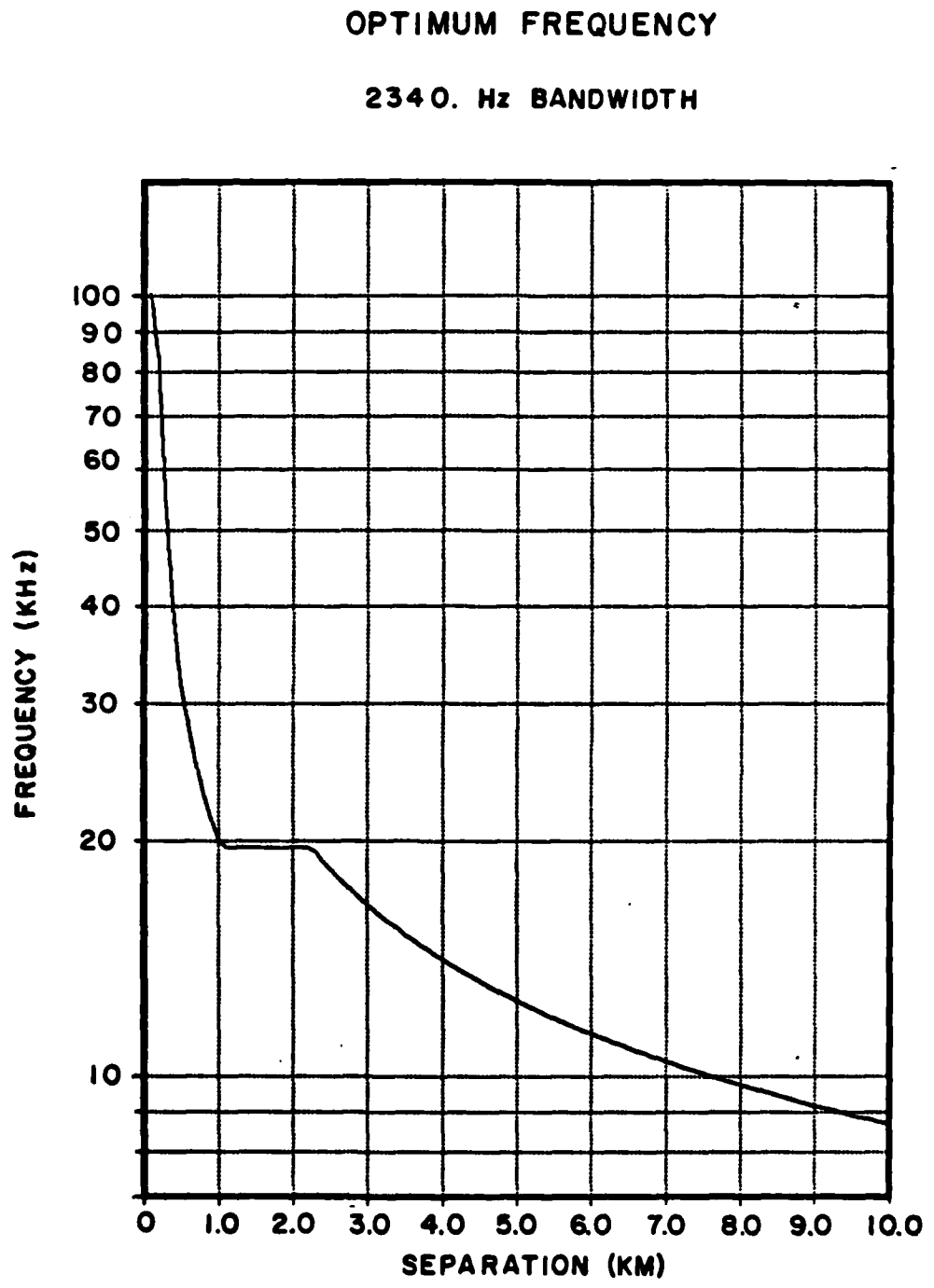


Figure 19 Optimum frequency as a function of range for a 0.5 watt link composed of a directional transmitter (15 cm maximum) and an omni-directional receiver operating at optimum frequency.

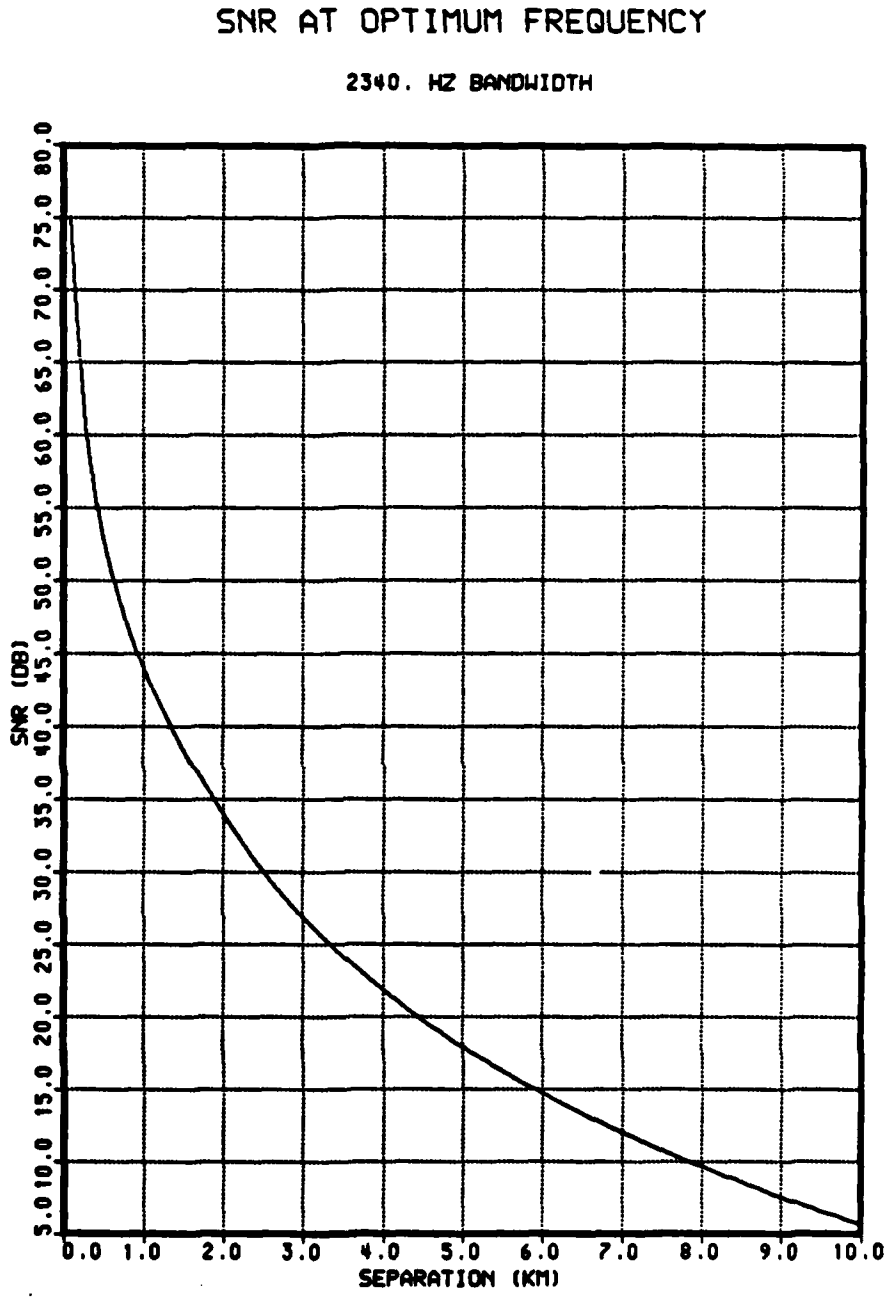


Figure 20 SNR as a function of range for a 0.5 watt link composed of a directional transmitter (15 cm maximum) and an omni-directional receiver operating at optimum frequency into a 2340 Hz (bandwidth) channel.

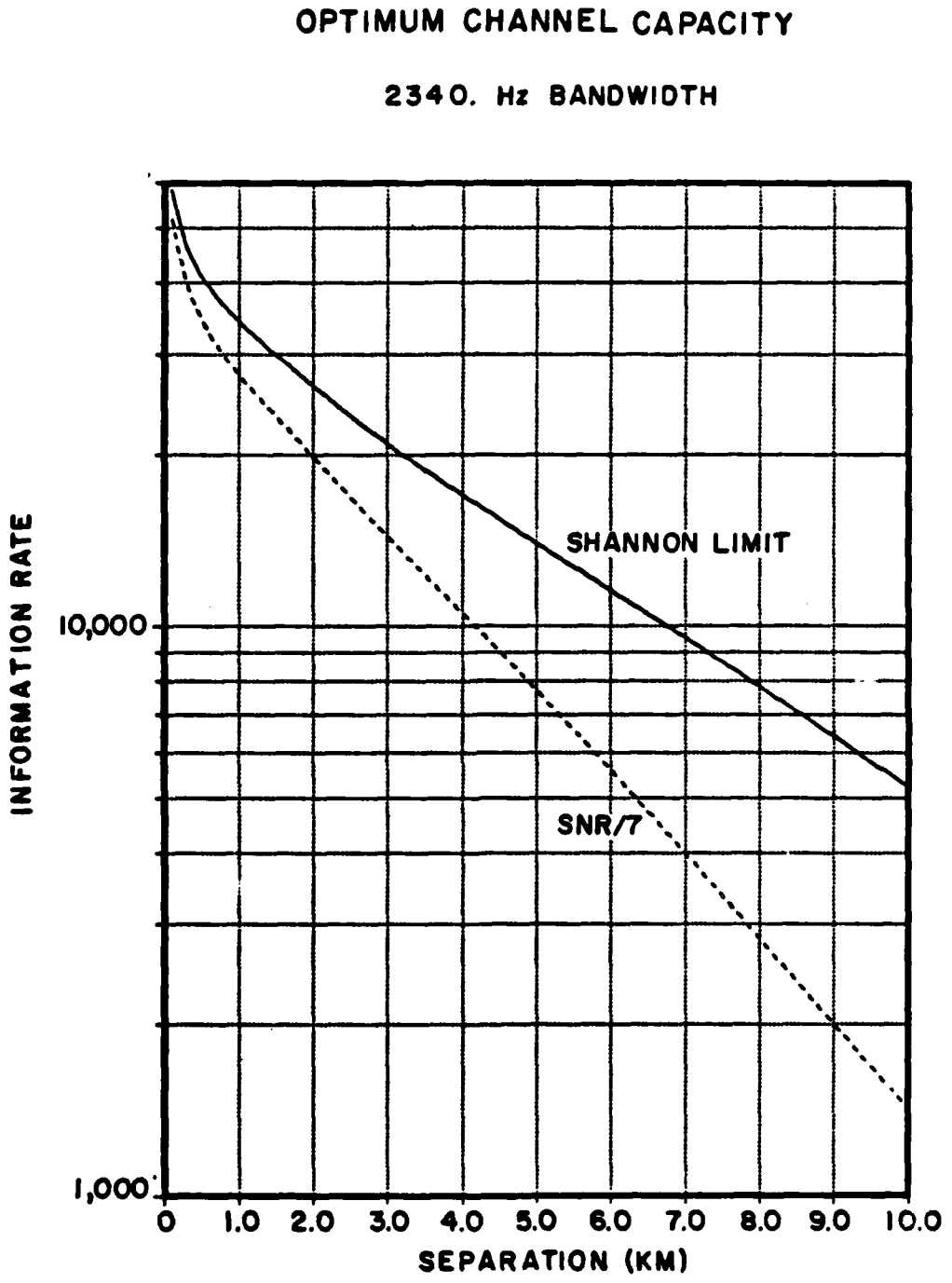


Figure 21 Shannon limit as a function of range for a 0.5 watt link composed of a directional transmitter (15 cm maximum) and an omni-directional receiver operating at optimum frequency into a 2340 Hz (bandwidth) channel.

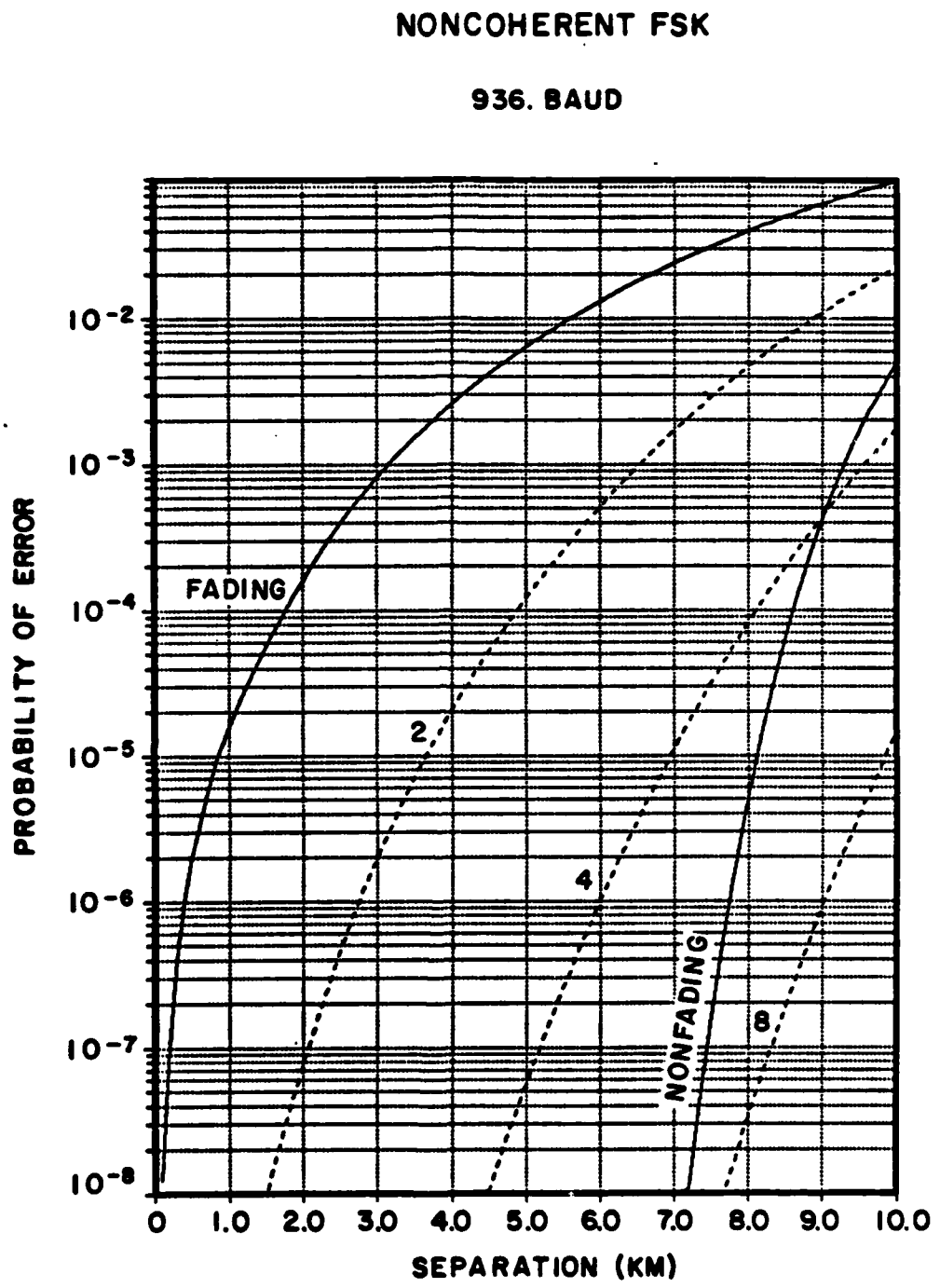


Figure 22 Noncoherent FSK probability of error as a function of range for a 0.5 watt link composed of a directional transmitter (15 cm maximum) and an omni-directional receiver operating at optimum frequency. The effects of fading and diversity are illustrated.

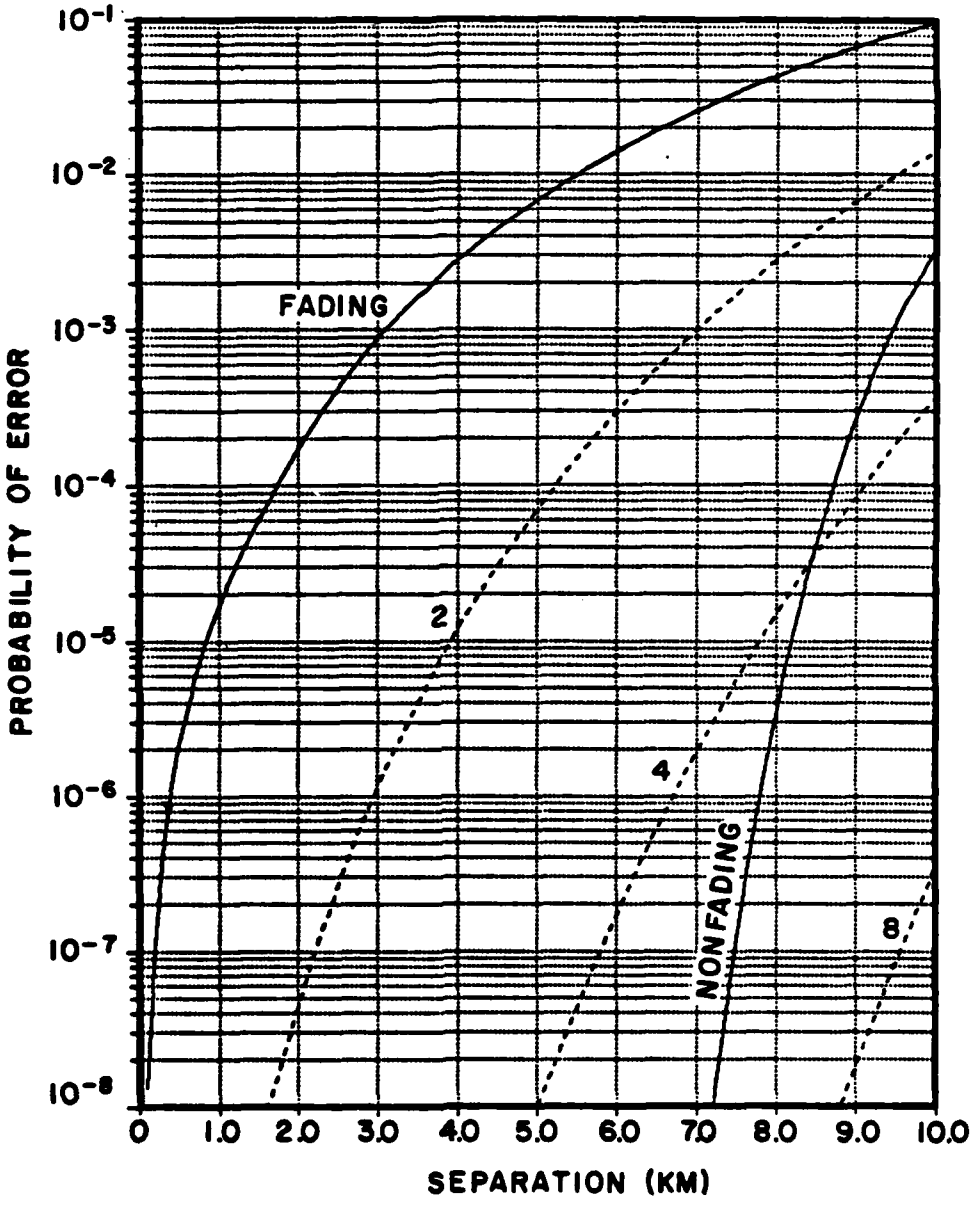


Figure 23 Coherent MSK (with maximal ratio combining) probability of error as a function of range for a 0.5 watt link composed of a directional transmitter (15 cm maximum) and an omni-directional receiver operating at optimum frequency. The effects of fading and diversity are illustrated.

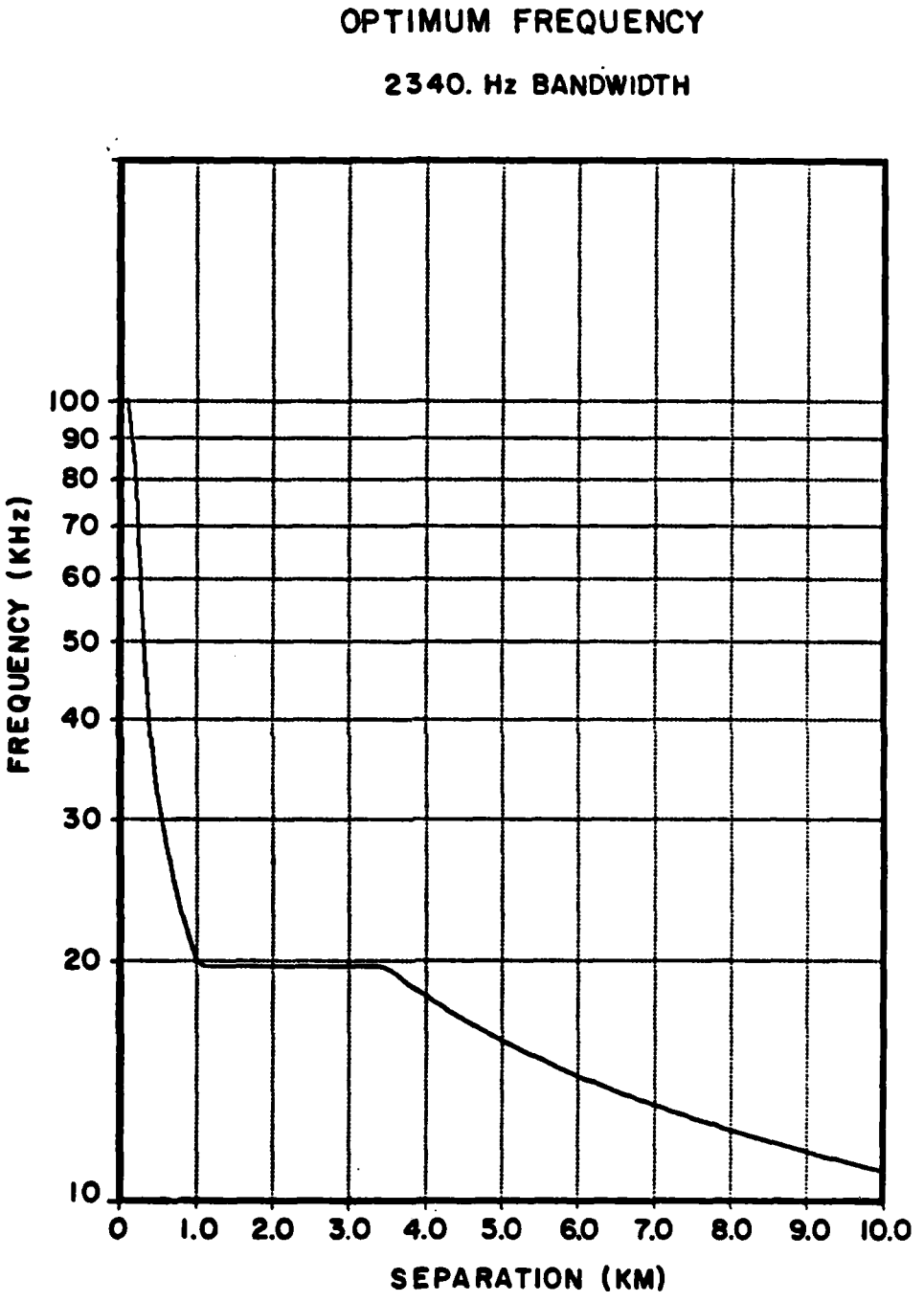


Figure 24 Optimum frequency as a function of range for a 0.5 watt link composed of a directional transmitter (15 cm maximum) and an identical receiver operating at optimum frequency.

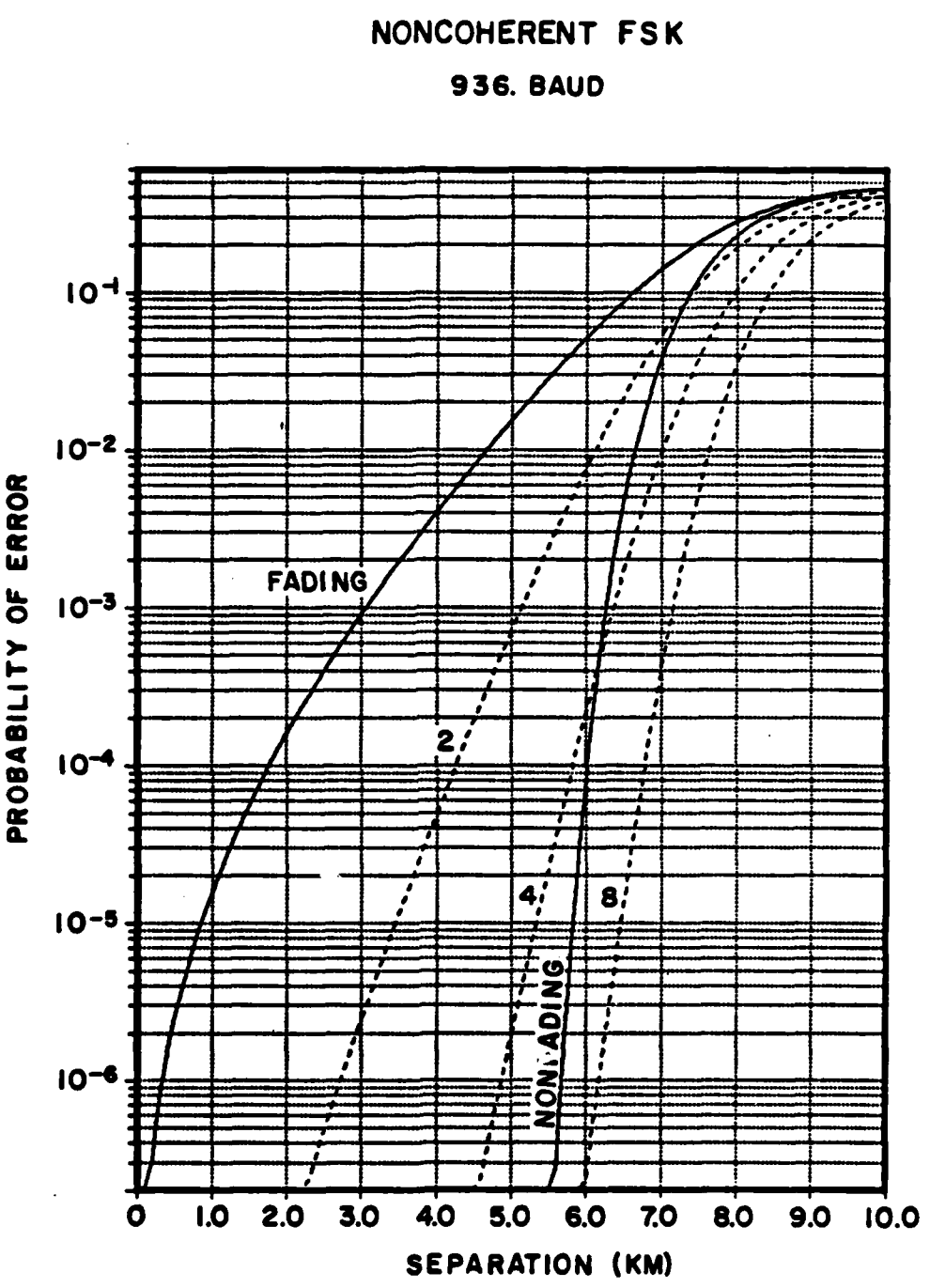


Figure 25 Noncoherent FSK probability of error as a function of range for a 0.5 watt link composed of a 15 cm transmitter and an omni-directional receiver operating at a fixed frequency of 19.67 kHz. The effects of fading and diversity are illustrated.

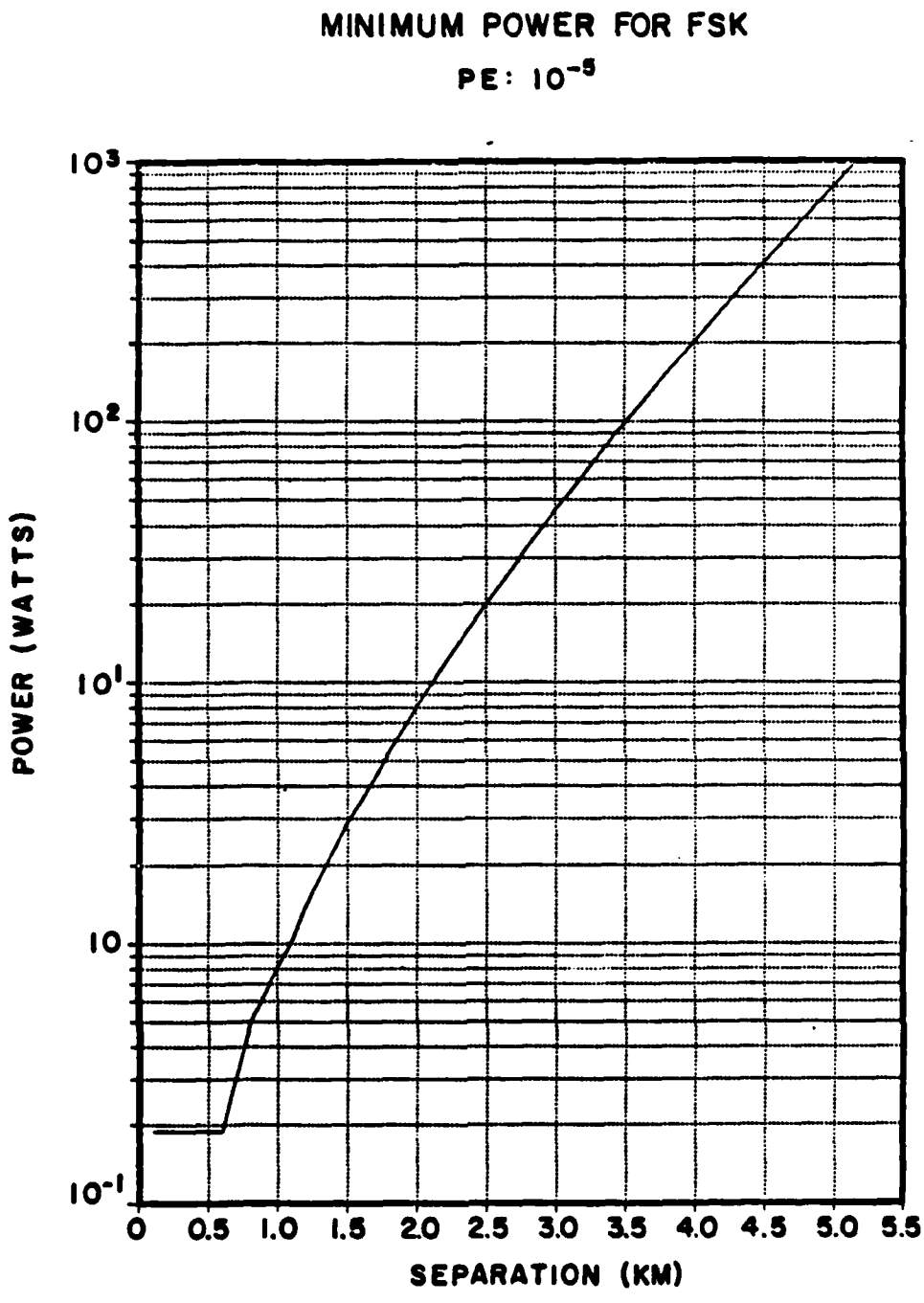


Figure 26 Power required for a noncoherent FSK BER of $10^{-5}$ as a function of range for a 0.5 watt link composed of a 15 cm transmitter and an omni-directional receiver operating at a fixed frequency of 19.67 kHz.

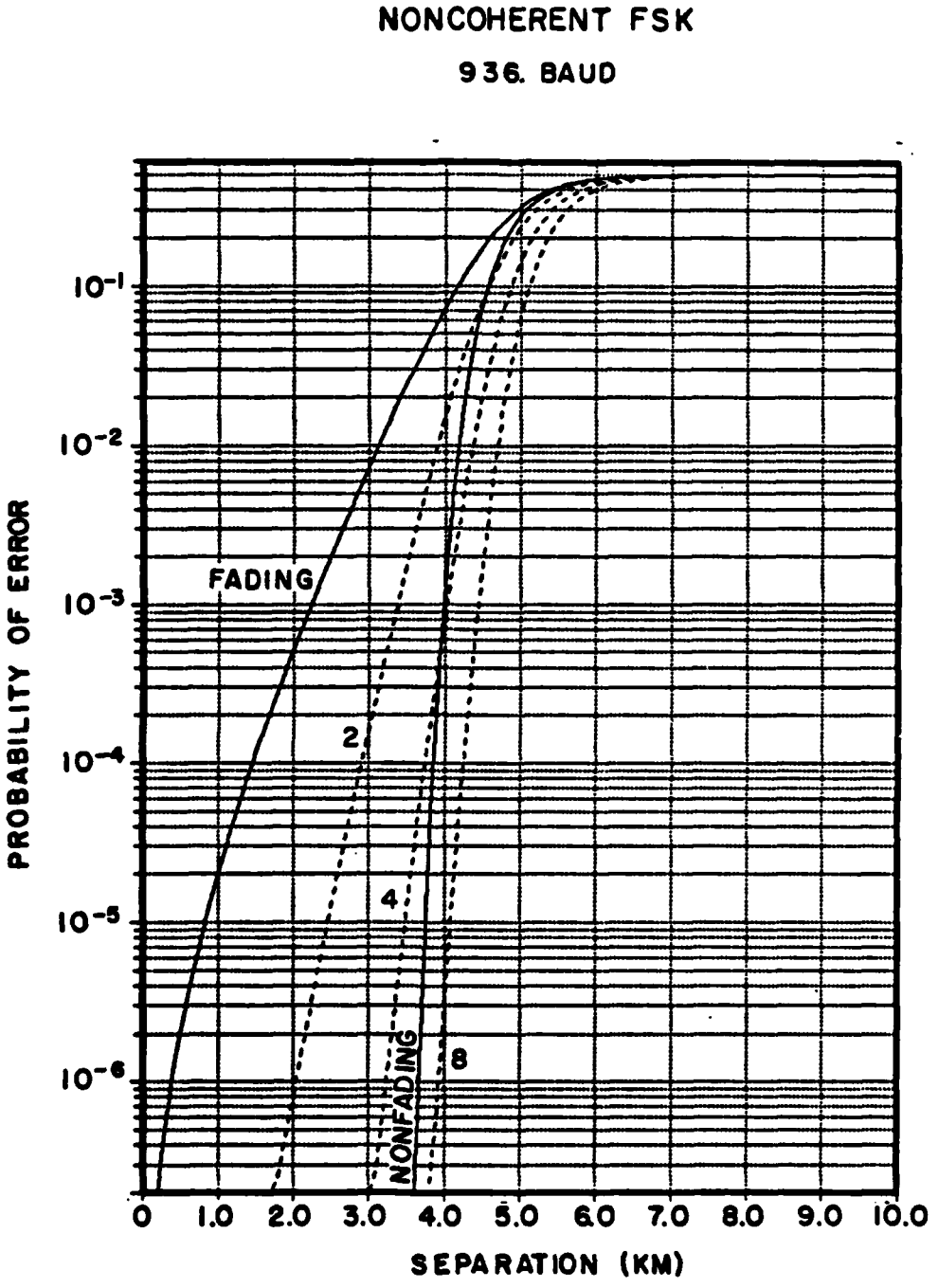


Figure 27 Noncoherent FSK probability of error as a function of range for a 0.5 watt link composed of a 10 cm transmitter and an omni-directional receiver operating at a fixed frequency of 29.5 kHz. The effects of fading and diversity are illustrated.

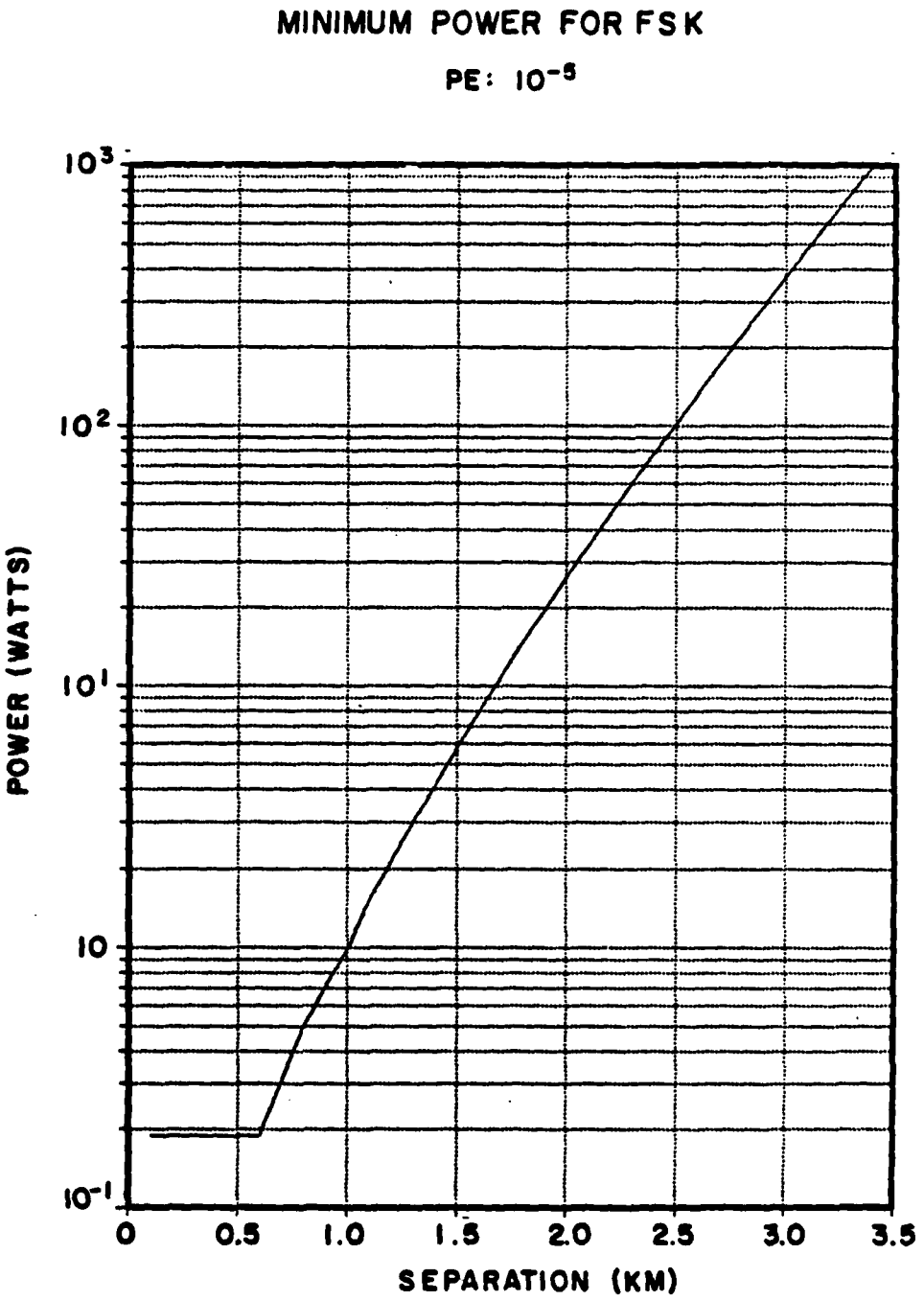


Figure 28 Power required for a noncoherent FSK BER of $10^{-5}$ as a function of range for a 0.5 watt link composed of a 10 cm transmitter and an omni-directional receiver operating at a fixed frequency of 29.5 kHz.

# OCEANO DT 122

- BI - DIRECTIONAL DIGITAL ACOUSTIC LINK
- 4 FREQUENCY FSK MODULATION
- OPERATIONAL IN SEA STATE 6 + 60 dB DRILL SHIP
- PEAK POWER TO TRANSMITTER - 375 WATTS
- BER AT SEA STATE 6 + 40 dB:

  1.5 km $8x10^{-42}$
  2.0 km $2x10^{-10}$
  3.0 km $8x10^{-7}$

- DATA RATE - 80 BITS/S
- BEAMWIDTH - 30 DEGREES

Figure 29 Some operating characteristics of the Oceano Instruments U.S.A., Inc. DT 122 Acoustic Data Transmission System.

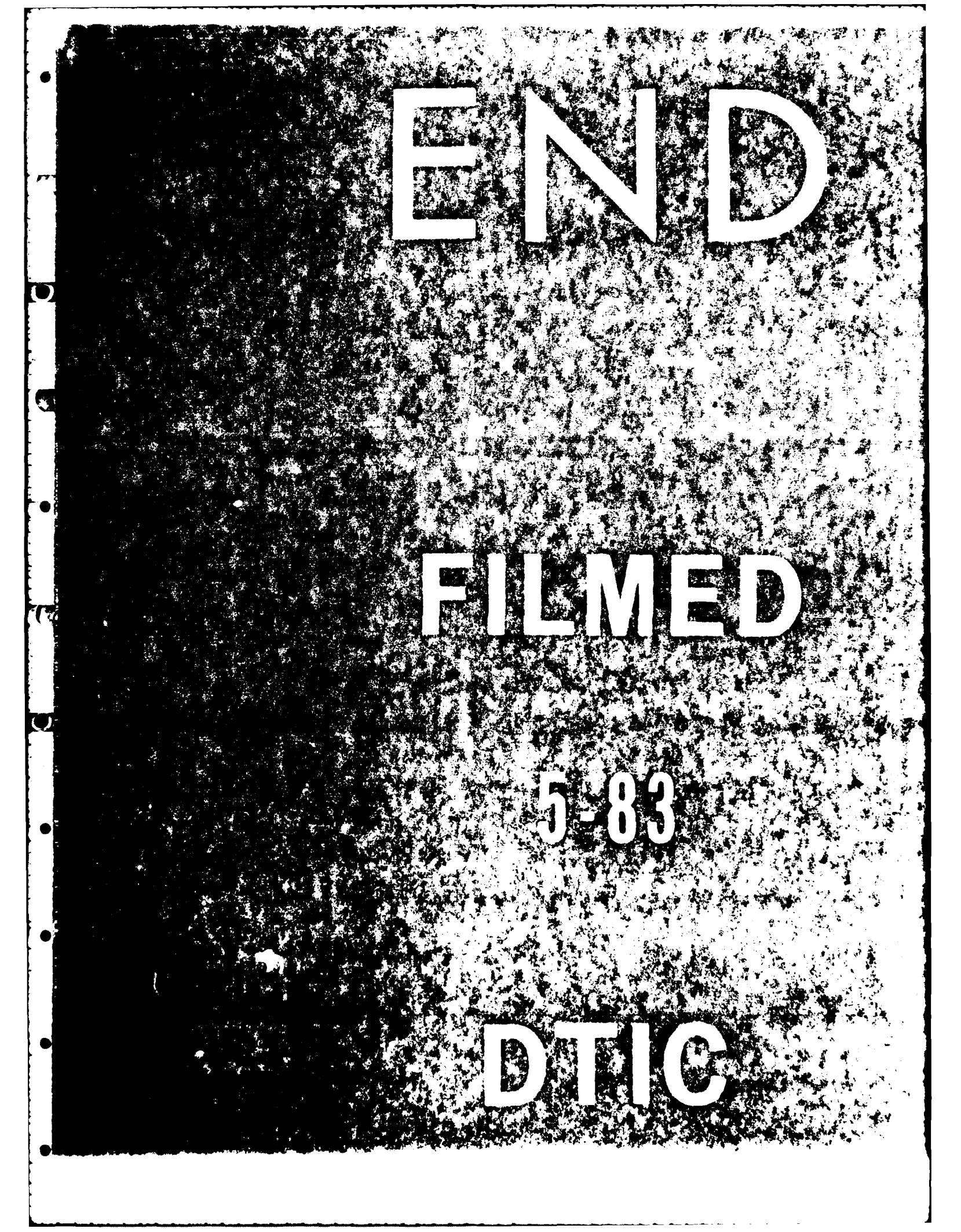
END
FILMED
5-83
DTIC